UNIVERSIDADE DE SÃO PAULO
FACULDADE DE MEDICINA

LAIZ LAURA DE GODOY

Biomarcadores de neuroimagem em superagers estudados por meio da ressonância magnética de crânio multimodal

São Paulo

2023

LAIZ LAURA DE GODOY

Biomarcadores de neuroimagem em superagers estudados por meio da ressonância magnética de crânio multimodal

Versão Original

Tese apresentada à Faculdade de Medicina da Universidade de São Paulo para obtenção do título de Doutor em Ciências

Programa de Radiologia

Orientadora: Profa. Dra. Claudia da Costa Leite

São Paulo

2023

Dados Internacionais de Catalogação na Publicação (CIP)

Preparada pela Biblioteca da
Faculdade de Medicina da Universidade de São Paulo

de Godoy, Laiz Laura
Biomarcadores de neuroimagem em superagers estudados por meio da ressonância magnética de crânio multimodal / Laiz Laura de Godoy. -- São Paulo, 2023.
Tese(doutorado)--Faculdade de Medicina da Universidade de São Paulo.
Programa de Radiologia.
Orientadora: Claudia da Costa Leite.

Descritores: 1.Superager 2.Memória 3.Cognição 4.Envelhecimento 5.Espectroscopia de prótons por ressonância magnética 6.Imagem por ressonância magnética funcional 7.Biomarcadores

USP/FM/DBD-453/23

Responsável: Erinalva da Conceição Batista, CRB-8 6755

Dedico esse trabalho aos meus pais,
à Cecília Camargo e ao Nelson Godoy.

AGRADECIMENTOS

A minha sincera gratidão àqueles que direta ou indiretamente contribuíram para a realização deste trabalho, seja através de orientação, incentivo, suporte ou carinho. Em um trabalho que estudo Super idosos eu tive o privilégio de ter Super pessoas ao meu lado.

Aos participantes idosos, que me encantaram por sua experiência, juventude, e prazer por viver. Eles são as verdadeiras estrelas desse trabalho de pós-graduação, que mudaram minha forma de ver a vida, e com quem pude fazer elos de amizade e carinho.

A minha orientadora Profa. Cláudia da Costa Leite, que não é apenas uma médica cientista competente, a frente do seu tempo, mas uma pessoa e mãe excepcional, em quem me inspiro. Me proporcionou estudar e desbravar um tópico único, pelo qual me apaixonei, me dando todo suporte e mentoria necessários.

Ao meu co-rientador da *University College London*, Dr. Sotirios Bisdas, que me abriu as portas de uma grande Universidade internacional com cientistas capacitados e tecnologia de ponta, para que eu pudesse analisar os dados de imagem obtidos na Universidade de São Paulo e concluir importantes publicações.

A minha banca de qualificação (Drs. Antonio Maia, Leandro Lucato, Cesar Alves) por suas excelentes sugestões e correções, que contribuíram para conclusão desta tese de doutorado.

Ao meu colega de trabalho e amigo, Cesar Alves, que me incentivou a fazer o doutorado, e me mostrou que eu tinha muitos capítulos de um livro para percorrer na minha carreira, e que eu seria capaz de grandes conquistas e superar os desafios.

À minha família, que sempre atenta e com amor, me deram o suporte mais precioso. Minha avó Laura, que não está mais aqui, mas sempre zelou por mim, uma avó carinhosa. Minha avó Adayr, um anjo, que ora incessantemente pela família e cuida de mim.

Em especial aos meus pais, que juntos são uma equipe para me ajudar. Meu pai, Nelson, que me ensinou ser uma pessoa honesta, batalhadora e corajosa. Não mediu esforços pelos meus objetivos e sonhos, me dando o suporte emocional e financeiro para que eu pudesse fazer grande parte da pós-graduação na Inglaterra. Meu herói, minha base forte. Minha mãe, Cecília, indissociável de mim como um reflexo. Está ao meu lado a cada segundo, me faz forte e feliz. Viveu cada instante dessa jornada, e é o pivô das minhas conquistas. Minha rainha, linda.

Deus, Jesus Cristo, o maestro da minha vida, quem me permitiu ser, quem determinou todos os meus passos desde meu primeiro instante de existência.

RESUMO

Godoy LL. Biomarcadores de neuroimagem em superagers estudados por meio da ressonância magnética de crânio multimodal [tese]. São Paulo: Faculdade de Medicina, Universidade de São Paulo; 2023.

Introdução: Superagers são amplamente definidos como indivíduos com mais de 80 anos com desempenho de memória episódica semelhante ou superior aos indivíduos de meia-idade (50-65 anos), o que pode refletir resiliência aos mecanismos convencionais do envelhecimento. Para oferecer um conhecimento mais abrangente sobre o fenótipo dos superagers, vários biomarcadores, incluindo testes neuropsicológicos, neuroimagem, perfis genéticos, histopatológicos e bioquímicos, têm sido estudados na última década. Em termos de registros de neuroimagem, sabe-se que os superagers mostram preservação cortical seletiva em regiões específicas da rede de modo padrão e rede de saliência, sobrepostos por conectividade funcional mais forte. No entanto, esses estudos incluíram indivíduos a partir dos 60 anos de idade, o que pode ser tendencioso para obter afirmações significativas sobre o desempenho da memória preservada no extremo da vida (≥ 80 anos). **Objetivos**: Explorar a importância dos biomarcadores de neuroimagem usando técnicas multimodais de ressonância magnética cerebral para caracterizar superagers e diferenciá-los de seus pares com envelhecimento cognitivo normal. Primeiro, procuramos investigar qualquer relação entre as concentrações de metabólitos cerebrais obtidos por espectroscopia de prótons de voxel único por RM no giro do cíngulo posterior, com o desempenho cognitivo em uma população selecionada de superagers e controles idosos cognitivamente normais (controles idosos). Nossa hipótese é que existe uma assinatura neuroquímica diferente entre esses dois grupos de participantes. Em um estudo adicional, comparamos as diferenças na conectividade funcional no estado de repouso entre superagers e controles idosos em uma variedade de redes neurais para identificar as redes mais discriminativas e as regiões dentro das redes capazes de prever os superagers. Além disso, examinamos as diferenças na probabilidade de ser um superager entre os dados de RM funcional em estado de repouso em campos magnéticos de 3 Teslas (T) e 7T. Nossa hipótese é que as redes funcionais são críticas para prever a função cognitiva preservada em superagers, e as medidas de conectividade funcional seriam aprimoradas em um campo magnético ultra alto. **Métodos:** Trata-se de uma compilação de dois artigos. Para o primeiro estudo, 25 participantes, compreendendo 12 superagers e 13 controles da mesma média de idade, foram analisados estatisticamente. Usamos espectroscopia de prótons de voxel único na RM 3T para quantificar 18 neurometabólitos no córtex do giro do cíngulo posterior de nossos participantes. Todos os dados da espectroscopia foram analisados usando o software LCModel. Os resultados foram posteriormente analisados usando duas abordagens para comprovar a precisão da técnica: i) comparação da concentração média de metabólitos estimada com limites inferiores de Cramer-Rao < 20%; ii) cálculo e comparação das médias ponderadas dos metabólitos. No segundo estudo, 31 participantes, compreendendo 14 superagers e 17 controles idosos, foram incluídos para análise. Os participantes foram submetidos a RM funcional de repouso em aparelhos de RM 3T e 7T. Um algoritmo de classificação de predição usando um modelo de regressão penalizado

nas medições da rede foi empregado para calcular as probabilidades de um idoso saudável ser um superager. Além disso, usamos Odds Ratios (ORs) para quantificar a influência de cada região (nós) em redes pré-selecionadas. **Resultados:** No estudo de espectroscopia, o principal achado observado foi uma maior concentração total de N-acetil aspartato (NAA+NAAG) em superagers do que em controles idosos usando ambas as técnicas ($p = 0,02$ para concentração média e $p = 0,03$ para as médias ponderadas). No estudo investigando a RM funcional em estado de repouso entre os grupos, as principais redes que diferenciaram superagers de controles idosos foram as redes de modo padrão, saliência e rede de linguagem. Os nós mais discriminativos (ORs > 1) em superagers abrangeram áreas no pré-cúneo do córtex cingulado posterior, córtex pré-frontal, junção temporoparietal, pólo temporal, córtex extraestriado superior e ínsula. O modelo de classificação de previsão para ser um superager mostrou melhor desempenho usando o conjunto de dados na RM funcional de repouso no aparelho 7T comparado ao 3T. **Discussão e Conclusão:** Esta compilação de artigos usando técnicas multimodais de RM cerebral pode contribuir como biomarcadores para diagnosticar o declínio cognitivo precoce e fornecer novos *insights* sobre os mecanismos biológicos envolvidos na resiliência cognitiva. O primeiro estudo destacou e comparou as diferenças metabólicas no córtex cingulado posterior de superagers e controles idosos, apontando para a direção de que concentrações mais altas de NAA total podem contribuir para o processo de resiliência das vias convencionais de envelhecimento presentes em superagers. No segundo estudo, nossos achados indicaram que a RM funcional de crânio em estado de repouso pode ser uma técnica útil para acessar memória preservada nos idosos e em identificar potenciais superagers, particularmente em regiões pertencentes às redes de modo padrão, saliência, e rede de linguagem. Nossos resultados também destacam o benefício dos aparelhos de RM de campo magnético 7T sobre o 3T para esta tarefa de diagnóstico e classificação, contando principalmente com o aumento da relação sinal-ruído temporal e os maiores coeficientes de conectividade funcional do estado de repouso fornecidos pelo campo ultra-alto. Nossos resultados garantem validação adicional em estudos prospectivos com coortes maiores.

Palavras-chave: Superager. Memória. Cognição. Envelhecimento. Espectroscopia de Prótons por Ressonância Magnética. Imagem por Ressonância Magnética Funcional. Biomarcadores.

ABSTRACT

Godoy LL. Neuroimaging biomarkers in superagers accessed by multimodal brain MRI [thesis]. São Paulo: "Faculdade de Medicina, Universidade de São Paulo"; 2023.

Introduction: Superagers are broadly defined as individuals over 80 years old with episodic memory performance similar or superior to middle-aged subjects (50–65 years old), which may reflect resilience to the conventional pathways of aging. To offer more comprehensive knowledge about the superagers phenotype, several biomarkers, including neuropsychological tests, neuroimaging, genetic, histopathological, and biochemical profiles, have been sought over the last decade. In terms of neuroimaging records, it is known that superagers show selective cortical preservation in particular regions of the default mode network (DMN) and salience network (SN), overlapped by stronger functional connectivity. However, these studies included subjects from 60 years old, which may be biased to obtain meaningful assertions about "youthful" memory performance in late life (≥ 80 years old). **Objectives:** To explore the significance of neuroimaging biomarkers using multimodal brain MRI techniques to characterize superagers and differentiate them from their normal aging peers. First, we sought to investigate any relationship between brain metabolite concentrations obtained by single-voxel proton magnetic resonance spectroscopy (^{1}H-MRS) placed in the posterior cingulate cortex with the cognitive performance in a selected population of superagers and cognitively average elderly controls (elderly controls). We hypothesized that there is a different neurochemical signature between these two subjects' groups. In an additional study, we compared the differences in the resting-state functional connectivity between superagers and elderly controls in a range of neural networks to identify the most discriminative networks and within-network nodes for predicting superagers. We additionally examined differences in the prediction probability of being a superager between the resting-state functional MRI (rs-fMRI) data at 3 Tesla (T) and 7T magnetic fields. We hypothesized that hub regions are critical to predicting youthful cognitive function in superagers, and the measurements of functional connectivity would be improved at a higher magnetic field. **Methods:** This is a compilation of two articles. For the first study, 25 participants, comprising 12 superagers and 13 age-matched controls, were statistically analyzed. We applied state-of-the-art 3 Tesla ^{1}H-MRS to quantify 18 neurochemicals in the posterior cingulate cortex of our subjects. All ^{1}H-MRS data were analyzed using LCModel. Results were further analyzed using two approaches to investigate the technique accuracy: i) comparison of the average concentration of metabolites estimated with Cramer-Rao lower bounds < 20%; ii) calculation and comparison of metabolites' weighted means. In the second study, 31 participants, comprising 14 superagers and 17 cognitively average elderly controls, were included for analysis. Participants underwent rs-fMRI at 3T and 7T MRI scanners. A prediction classification algorithm using a penalized regression model on the network's measurements was employed to calculate the probabilities of a healthy older adult being a superager. Additionally, Odds Ratios (ORs) quantified the influence of each node across pre-selected networks. **Results:** In the ^{1}H-MRS study, the main finding observed was a higher total *N*- acetyl

aspartate (NAA+NAAG) concentration in superagers than in elderly controls using both approaches ($p = 0.02$ for average concentration and $p = 0.03$ for the weighted means). In the rs-fMRI study, the key networks that differentiated superagers and elderly controls were the DMN, SN, and language networks. The most discriminative nodes (ORs >1) in superagers encompassed areas in the precuneus posterior cingulate cortex, prefrontal cortex, temporoparietal junction, temporal pole, extrastriate superior cortex, and insula. The prediction classification model for being a superager showed better performance using the 7T over 3T rs-fMRI dataset. **Discussion and Conclusion:** This compilation of articles using multimodal brain MRI techniques could assist as surrogate biomarkers for diagnosing early cognitive decline and provide novel insights into the biological mechanisms involved in cognitive resilience. The first study highlighted and compared the metabolic differences in the posterior cingulate cortex of superagers and elderly controls pointing to the direction that higher concentrations of total NAA can contribute to the resilience process of the conventional pathways of aging present in superagers. In the second study, our findings indicated that rs-fMRI might be a useful technique in assessing youthful memory performance in late life and identifying potential superagers, particularly in nodes among the DMN, SN, and language network. Our results highlight the benefit of 7T over the 3T magnetic field scanners for this diagnostic and classification task, mainly relying on the increased temporal signal-to-noise ratio (SNR) and resting state functional connectivity coefficients provided by ultra-high field. Our results warrant further validation in larger prospective studies.

Keywords: Superager. Memory. Cognition. Aging. Proton Magnetic Resonance Spectroscopy. Functional Resonance Magnetic Imaging. Biomarkers.

LISTA DE FIGURAS

ARTIGO 1

ARTIGO 2

LISTA DE TABELAS

ARTIGO 1

ARTIGO 2

LISTA DE ABREVIATURAS

^{1}H-MRS	espectroscopia de prótons por ressonância magnética
Cho	colina
Cr	creatina
CRLB	limites inferiores de Cramer-Rao
CSF	liquido cefaloraquidiano
DMN	rede de modo padrão
ECN-L	rede de controle executivo à esquerda
ECN-R	rede de controle executivo à direta
Glu	glutamato
mI	mio-inositol
MMSE	mini exame do estado mental
MoCA	avaliação cognitiva de Montreal
MRI	ressonância magnética
NAA	*N*- acetil aspartato
NAAG	*N*-acetil aspartil glutamato
OR	odds ratio
RM	ressonância magnética
rs-fMRI	RM funcional em estado de repouso (*resting state)*
SD	desvio padrão
SN	rede saliência
SNR	razão sinal ruído
T	Tesla

ABBREVIATIONS OF FIGURE 3 – ARTICLE 2

Cingp	posterior cingulate cortex.
ContA	control A.
ContB	control B.
ContC	control C.
DMN	default mode network.

DorsAttnA	dorsal attention A.
DorsAttnB	dorsal attention B.
ExStrSup	extra-striate superior cortex.
FrMed	frontal medial cortex.
Ins	Insula.
IPL	inferior parietal lobule.
IPS	intraparietal sulcus.
LH	left hemisphere.
OFC	orbital frontal cortex.
ParOper	parietal operculum.
PCC	Precuneus posterior cingulate cortex.
pCun	precuneus.
PHC	parahippocampal cortex.
PFCd	dorsal prefrontal cortex.
PFCl	lateral prefrontal cortex.
PFClv	lateral ventral prefrontal cortex.
PFCm	medial prefrontal cortex.
PFCmp	medial posterior prefrontal cortex.
PFCv	ventral prefrontal cortex.
PostC	postcentral cortex.
RH	right hemisphere.
Rsp	retrosplenial cortex.
SalVentAttnA	salience / ventral attention A.
SalVentAttnB	salience / ventral attention B.
SPL	superior parietal lobule.
Temp	temporal cortex.
TempPar	temporoparietal junction.
TempPole	medial temporal pole.
TempOcc	temporo-occipital junction.
VisPeri	peripheral visual.

LISTA DE SIGLAS

FMUSP	Faculdade de Medicina da Universidade de São Paulo
HCFMUSP	Hospital das Clínicas da Faculdade de Medicina da Universidade de São Paulo
InRad	Instituto de Radiologia

SUMÁRIO

1 INTRODUÇÃO

1 INTRODUÇÃO

1.1 IDOSOS COM MEMÓRIA EXCEPCIONAL (SUPERIDOSOS OU "SUPERAGERS")

O senso comum nos leva à concepção que o declínio cognitivo é um processo natural e inexorável ao envelhecimento normal, mesmo entre aqueles que não progridem para comprometimento cognitivo leve ou demência. No entanto, a partir de observações de idosos cujas habilidades cognitivas mantém-se estável a despeito do envelhecimento, criou-se o termo "superidosos" (ou "*SuperAgers*") [1–4]. O grupo liderado pelo professor M.-Marcel Mesulam definiu os superagers como idosos octa e nonagenários cujo desempenho em testes de memória episódica está acima dos padrões normatizados para idade e com valores correspondente a indivíduos 20 a 30 anos mais jovens. Além disso, o desempenho dos superagers em outras funções cognitivas não relacionadas a memória, deve estar dentro ou acima de um desvio padrão (DP) da média para sua idade e dados demográficos [1]. E este foi o critério adotado no nosso estudo para a classificação dos superagers.

Em um seguimento longitudinal por 18 meses, um grupo de idosos classificados como superagers não apresentou declínio cognitivo, não apenas no domínio de memória, como também em outros domínios cognitivos [2]. Esse grupo havia sido inicialmente submetido à morfometria cortical por voxel em ressonância magnética (RM) e foram comparados com indivíduos de 50 a 65 anos. Interessantemente, não se encontrou atrofia cortical significativa no grupo dos superagers, bem como estes apresentavam uma espessura cortical maior na região anterior do giro do cíngulo direito, comparado com controles idosos bem como com adultos de meia-idade (50-60 anos) [4].

A revisão sistemática do nosso grupo [5], incluindo 21 artigos sobre superagers, observou principalmente uma preservação cortical seletiva em superagers comparada com controles idosos da mesma média de idade, em regiões pertencentes a rede de

modo padrão (DMN) e rede de saliência (SN), incluindo o giro do cíngulo anterior, hipocampo, córtex pré-frontal, e ínsula, à despeito de uma preservação cortical global [6–11]. Sobrepondo a integridade estrutural dos superagers, algumas regiões do DMN e SN também apresentaram conectividade funcional mais forte em superagers, destacando possíveis nós (*hubs*) importantes para memória e cognição [12,13]. Em relação aos estudos de PET amiloide, os níveis de deposição de amilóide não foram significativamente diferentes entre superagers e controles da mesma idade, apontando para uma potencial resiliência cerebral nos superagers no que se refere a neurodegeneração [7,9,10,14].

Ainda sobre os resultados da revisão sistemática [5], em estudos *post-mortem* de idosos com capacidade cognitiva excepcional, foi notada uma menor frequência de emaranhados neurofibrilares do tipo Alzheimer e uma maior densidade de neurônios de von Economo no giro do cíngulo anterior [4,15]. Com relação aos estudos genéticos, as diferenças entre superagers e controles idosos ainda estão sendo debatidas em relação à importância do alelo ε4 da APOE e nenhuma conclusão foi obtida até o momento [5]. Porém, foi observado que o perfil superager está associado a variantes no gene *MAP2K3*, o qual pertence a uma cascata de sinalização relacionada com apoptose beta-amilóide mediada [16].

Há um relativo pequeno número de estudos publicados analisando os superagers e quais seriam os fatores de maior resiliência desses indivíduos às mudanças associadas ao envelhecimento normal e às patologias neurodegenerativas. Além disso, não há consenso entre os pesquisadores quanto aos instrumentos e critérios mais adequados para classificação dos superagers. Por exemplo entre os estudos publicados no tópico, há variações nos testes neuropsicológicos (memória e funções cognitivas) empregados, idade mínima de inclusão (60 versus 80 anos), e uso de grupo de adultos jovens ou apenas grupo de idosos cognitivamente normais para comparação com os resultados dos superagers. Em consequência, a falta de consenso sobre os instrumentos e critérios empregados na classificação dos superagers dificulta a comparação dos resultados entre os artigos científicos e pode introduzir viés na elaboração de conclusões assertivas sobre o desempenho da memória superior na vida tardia (≥ 80 anos).[5]

1.2 CONCEITOS DE RESERVA E MANUTENÇÃO CEREBRAL

As diferenças entre os indivíduos em relação ao desempenho cognitivo e de memória dependem de dois conceitos principais: (1) reserva [17] e (2) manutenção do cérebro [18]. (1) A reserva cerebral funciona como um mediador entre a patologia e o desfecho clínico. Pode ser convenientemente dividida em reserva cerebral, o modelo passivo, e reserva cognitiva, o modelo ativo. A Reserva cerebral refere-se a diferenças quantitativas no próprio cérebro, como cérebros com volume maior ou um número maior de neurônios, o que permite que alguns indivíduos tolerem melhor a patologia cerebral (por exemplo, peptídeo beta amiloide e proteína tau). Assim, um cérebro com maior espessura cortical pode ser capaz de suportar os efeitos patológicos antes que um limite crítico da reserva cerebral seja alcançado e o comprometimento da memória aconteça. Por outro lado, a reserva cognitiva representa uma forma de reserva dinâmica e qualitativa baseada na experiência e exposição ambiental desenvolvida ao longo da vida determinando conexões funcionais mais fortes [19,20]. Este conceito baseia-se principalmente nos processos cognitivos das redes funcionais cerebrais e no seu funcionamento adequado para lidar com a patologia cerebral, em vez da simples quantidade de neurônios e sinapses em uma determinada região do cérebro. Dentre os marcadores indiretos da reserva cognitiva, podemos citar o Quociente de Inteligência, anos de escolaridade, histórico profissional e o nível de envolvimento em atividades de lazer e culturais [21]. Assim, indivíduos com a mesma reserva cerebral, por exemplo, medida pelo volume total do cérebro, podem apresentar diferentes graus de reserva cognitiva adquirida ao longo da vida [22].

O conceito de (2) manutenção do cérebro é introduzido como um conceito complementar, que implica resistência a mudanças estruturais, funcionais e neuroquímicas ao longo dos anos. Ou seja, enquanto o conceito de reserva procura explicar porque alguns indivíduos apresentam funcionamento intacto na presença de patologia cerebral (peptídeo beta amiloide e proteína tau), o conceito de manutenção centra-se nas condições que promovem a preservação da integridade global do cérebro senescente. Assim, o foco está na relativa falta ou adiamento de alterações

cerebrais senescentes, incluindo neuropatologia, e não nas formas de lidar com a sua presença. A manutenção cerebral é definida da seguinte forma, as diferenças individuais na manifestação das alterações estruturais cerebrais e neuropatológicas relacionadas com a idade permitem que algumas pessoas apresentem pouco ou nenhum declínio cognitivo relacionado com a idade [18].

De acordo com a hipótese de manutenção, a minimização das alterações cerebrais senescentes e a ausência de patologia são os melhores preditores do desenvolvimento bem-sucedido da memória na velhice. Dois padrões de evidência apoiariam a utilidade desta hipótese para explicar diferenças individuais no envelhecimento da memória. Em primeiro lugar, espera-se que os indivíduos idosos difiram amplamente na quantidade de alterações cerebrais neuroquímicas, estruturais e funcionais que apresentam. Em segundo lugar, o conceito assume uma associação positiva entre perdas cerebrais e cognitivas graduadas pela idade: indivíduos que apresentam menos perdas nas propriedades cerebrais relacionadas com tarefas apresentarão menor declínio no desempenho da memória.

Os superagers dessa forma emergem como uma população valiosa porque podem atuar como um modelo para elucidar os mecanismos cerebrais subjacentes a preservação da memória na velhice, o que pode explicar as teorias da reserva e da manutenção do cérebro.

1.3 A IMPORTÂNCIA DA RM MULTIPARAMÉTRICA E ALTO CAMPO MAGNÉTICO PARA CARACTERIZAÇÃO DOS SUPERAGERS

Achados sutis e precoces de declínio cognitivo são ocultos no estudo de RM de crânio convencional. Com o objetivo de entender os achados metabólicos e fisiológicos dos superagers, o uso de técnicas de neuroimagem avançada, como a espectroscopia de prótons por RM, RM funcional, e estudo dos tratos de substância branca por meio de DTI (*diffusion tensor imaging*) tem o potencial de contribuir como biomarcadores para diagnosticar o declínio cognitivo precoce e fornecer novos *insights* sobre os mecanismos biológicos envolvidos na resiliência cognitiva.

Biomarcadores são medidas quantificáveis de qualquer processo biológico (celular, genético, metabólico) que estão relacionados a parâmetros clínicos e, portanto, podem ser utilizados como substitutos diagnósticos e para acompanhamento de doenças. Por exemplo, os biomarcadores de neuroimagem têm papel potencial no diagnóstico precoce, bem como no acompanhamento periódico de doenças neurodegenerativas, como a doença de Alzheimer.

A espectroscopia de prótons por RM, que analisa de forma não invasiva vários metabólitos cerebrais, pode ser usada para fornecer informações sobre as vias bioquímicas associadas ao estado cognitivo do cérebro no envelhecimento [23]. Estudos anteriores relataram a correlação entre os parâmetros de concentração de metabólitos pela espectroscopia com medidas de inteligência [24–26], afeto [27], criatividade [28] e personalidade [29] em coortes de humanos normais. Tais descobertas sugerem que os neurometabólitos podem estar envolvidos em trajetórias saudáveis de envelhecimento cerebral, como as observadas entre os superagers.

As alterações fisiológicas do envelhecimento envolvem mecanismos celulares específicos, como bioenergéticos, estresse oxidativo, inflamação, renovação da membrana celular e neuroproteção endógena revelada por neurometabólitos na espectroscopia [30]. No geral, o cérebro envelhecido apresenta uma concentração reduzida de N-acetil aspartato (NAA) e glutamato (Glu) e uma concentração aumentada de colina (Cho) e Mio-inositol (mI) [31]. Alguns estudos mostraram correlação positiva entre concentração de NAA e melhor desempenho de memória em idosos saudáveis [31]. No entanto, não há estudos para determinar se essas alterações metabólicas relacionadas à idade se correlacionam com o desempenho neuropsicológico em superagers usando grupo controle com a mesma média de idade para comparação.

A RM funcional em estado de repouso (rs-fMRI) concentra-se nas características temporais e na organização espacial das flutuações espontâneas do sinal dependente do nível de oxigênio no sangue (BOLD) e é uma ferramenta poderosa para caracterizar a organização cerebral e suas anormalidades. Uma vez que as discrepâncias entre superagers e controles idosos cognitivamente normais podem ser modestas, mas importantes para detectar alterações precoces na função

cerebral, usar a RM funcional em estado de repouso em aparelhos de RM de campo magnético ultra alto, possibilitaria maior resolução espacial e temporal, permitindo a detecção de alterações mais sutis [32].

Nos últimos anos, a RM funcional para prática clínica no campo magnético 7T está ganhando força [33], pois oferece uma relação sinal-ruído benéfica e aumento do contraste BOLD em relação aos aparelhos convencionais de RM (1,5T e 3T) [34,35], traduzido em uma resolução espacial bastante aprimorada de atividade funcional, a principal vantagem técnica da RM funcional no campo 7T [35,36]. Um estudo prévio [37] demonstrou uma melhora de até 300% na relação sinal-ruído temporal e nos coeficientes de conectividade funcional do estado de repouso fornecidos pelo ultra alto campo 7T em comparação com o 3T, indicando maior poder para a detecção de arquitetura neural funcional. Acreditamos que o maior contraste BOLD para a relação de ruído disponível em 7T pode render melhor sensibilidade na detecção de diferenças na atividade nas redes cerebrais em comparação com o campo magnético 3T. Essas diferenças implicam que os aparelhos de RM 7T podem facilitar medições de conectividade com alta qualidade, capturando respostas evocadas em redes funcionais com maior robustez, oferecendo, portanto, um poder potencialmente maior em nível de grupo.

1.4 MOTIVAÇÃO

Mecanismos neurobiológicos multifatoriais parecem corroborar o complexo fenômeno do desempenho cognitivo excepcional em idosos. Os superagers emergem como uma população valiosa porque representam um modelo potencialmente capaz de esclarecer os mecanismos cerebrais subjacentes à resiliência cognitiva. Parâmetros de imagem fisiológicos e metabólicos por meio de técnicas avançadas de RM podem trazer informações cruciais para o entendimento desses sujeitos *in vivo*.

Uma vez que o envelhecimento é um fenômeno cada vez mais global, geralmente acompanhado de declínio cognitivo, com implicações diretas no sistema de saúde e na constituição da sociedade, há uma necessidade imperiosa de desenvolver biomarcadores robustos e quantitativos para avaliar de forma confiável e

dinâmica alterações sutis e precoces na cognição. A neuroimagem desponta como uma ferramenta amplamente disponível e não invasiva para essa investigação.

2 OBJETIVOS

2 OBJETIVOS

2.1 OBJETIVO PRIMÁRIO

- Explorar a RM de crânio multiparamétrica como potencial biomarcador de superagers, de forma a entender os mecanismos metabólicos e fisiológicos relacionados ao complexo fenômeno do envelhecimento com preservação da memória e cognição.

2.2 OBJETIVOS SECUNDÁRIOS

- Investigar a relação entre as concentrações de metabólitos cerebrais obtidos pela espectroscopia de prótons de voxel único por RM no giro do cíngulo posterior com o desempenho cognitivo em uma população selecionada de superagers e controles idosos cognitivamente normais.

- Comparar as diferenças na conectividade funcional no estado de repouso entre superagers e controles idosos cognitivamente normais em uma variedade de redes neurais com o objetivo de identificar as redes mais discriminativas. Examinar as diferenças na sensibilidade da RM funcional de repouso nos campos magnéticos 3T e 7T para detectar diferenças na atividade neural funcional entre os grupos e consequentemente a possibilidade de detectar um padrão para o superager.

3 DESENVOLVIMENTO E RESULTADOS

3 DESENVOLVIMENTO E RESULTADOS

O texto sistematizado se refere aos seguintes artigos originais conforme os objetivos da tese:

3.1 Artigo 1

1. Título: The brain metabolic signature in superagers using in vivo proton magnetic resonance spectroscopy: A pilot study.
2. Objetivo: **Investigar e comparar as diferenças metabólicas no giro do cíngulo posterior entre superagers e controles idosos cognitivamente normais, a fim de encontrar associações entre o desempenho excepcional de memória e os neurometabólitos detectados pela espectroscopia de prótons por RM.**
3. Revista: American Journal of Radiology (AJNR).

3.2 Artigo 2

4. Título: Phenotyping superagers by using resting-state functional magnetic resonance imaging.
5. Objetivo: **Investigar as redes neurais mais discriminativas e as principais diferenças entre as regiões pertencentes a cada rede entre superagers e controles idosos através da RM funcional de repouso. Examinar as diferenças na sensibilidade da RM funcional de repouso nos campos magnéticos 3T e 7T para detectar diferenças na atividade neural funcional entre os grupos e determinar se existe um padrão que possa estar relacionado ao grupo superager.**
6. Revista: American Journal of Radiology (AJNR).

3.1 ARTIGO 1

Title: The brain metabolic signature in superagers using in vivo proton magnetic resonance spectroscopy: a pilot study.

Running Title: *The brain metabolic signature in superagers using ^{1}H-MRS*

Authors:

Name	Orcid
Laiz L. de Godoy[1,4]	0000-0001-5956-5741
Adalberto Studart-Neto[2]	0000-0003-2260-5986
Marzena Wylezinska-Arridge[4]	0000-0002-2361-1029
Miriam Harumi Tsunemi[5]	0000-0002-9585-4230
Natália Cristina Moraes[2]	0000-0002-8439-6828
Mônica Sanches Yassuda[2]	0000-0002-9182-2450
Artur M. Coutinho[3]	0000-0002-5555-4583
Carlos A. Buchpiguel[3]	0000-0003-0956-2790
Ricardo Nitrini[2]	0000-0002-5721-1525
Sotirios Bisdas[4]	0000-0001-9930-5549
Claudia da Costa Leite1	0000-0002-1168-0780

Institutions:

[1] Department of Radiology and Oncology, Hospital das Clínicas, Faculdade de Medicina FMUSP, Universidade de Sao Paulo, Sao Paulo, 05403-000, São Paulo, SP, Brazil (BR).

[2] Department of Neurology, Hospital das Clínicas, Faculdade de Medicina FMUSP, Universidade de São Paulo, Sao Paulo, 05403-000, São Paulo, SP, Brazil (BR).

[3] Division and Laboratory of Nuclear Medicine (LIM 43), Department of Radiology and Oncology, Hospital das Clínicas, Faculdade de Medicina FMUSP, Universidade de São Paulo, 05403-000, São Paulo, SP, Brazil (BR).

[4] Department of Neuroradiology. The National Hospital of Neurology and Neurosurgery, University College London, WC1N 3BG, London, United Kingdom (UK).

[5] Department of Biostatistics, Institute of Biosciences, Universidade Estadual Paulista, 18618-970, Botucatu, São Paulo, SP, Brazil (BR).

Correspondence to:
Laiz Laura de Godoy.
Research fellow. The National Hospital of Neurology and Neurosurgery, University College London, London, United Kingdom.
Address: Queen Square, Holborn, London WC1N 3G, UK.

Telephone: +44 (0) 7391 783696
E-mail: laizlgodoy@gmail.com

Authors' Contributions:

Laiz L. Godoy: Study concept and design; Interpretation and analysis of the imaging data; main manuscript drafting and revision.

Adalberto Studart-Neto: Interpretation and collection of the clinical data; collection of the imaging data; manuscript drafting and revision.

Marzena Wilezinska-Arridge: Interpretation and analysis of the imaging data; manuscript drafting and revision.

Miriam Harumi Tsunemi: Responsible for the statistical analysis; manuscript drafting and revision.

Natália Cristina Moraes: Interpretation and collection of the clinical data; manuscript revision.

Mônica Sanches Yassuda: Interpretation and collection of the clinical data; manuscript revision.

Artur M. Coutinho: Collection of the imaging data; manuscript drafting and revision.

Carlos A. Buchpiguel: Collection of the imaging data; manuscript revision.

Ricardo Nitrini: Interpretation and collection of the clinical data; Collection of the imaging data; manuscript revision.

Sotirios Bisdas: Study concept and design; main manuscript drafting and revision.

Claudia da Costa Leite: Study concept and design; main manuscript drafting and revision; project administration.

MeSH Terms: Keywords: superagers; metabolites; ^{1}H-MRS; aging; memory

ORIGINAL RESEARCH
ADULT BRAIN

The Brain Metabolic Signature in Superagers Using In Vivo ^{1}H-MRS: A Pilot Study

L.L. de Godoy, A. Studart-Neto, M. Wylezinska-Arridge, M.H. Tsunemi, N.C. Moraes, M.S. Yassuda, A.M. Coutinho, C.A. Buchpiguel, R. Nitrini, S. Bisdas, and C. da Costa Leite

ABSTRACT

BACKGROUND AND PURPOSE: Youthful memory performance in older adults may reflect an underlying resilience to the conventional pathways of aging. Subjects having this unusual characteristic have been recently termed "superagers." This study aimed to explore the significance of imaging biomarkers acquired by ^{1}H-MRS to characterize superagers and to differentiate them from their normal-aging peers.

MATERIALS AND METHODS: Fifty-five patients older than 80 years of age were screened using a detailed neuropsychological protocol, and 25 participants, comprising 12 superagers and 13 age-matched controls, were statistically analyzed. We used state-of-the-art 3T ^{1}H-MR spectroscopy to quantify 18 neurochemicals in the posterior cingulate cortex of our subjects. All ^{1}H-MR spectroscopy data were analyzed using LCModel. Results were further processed using 2 approaches to investigate the technique accuracy: 1) comparison of the average concentration of metabolites estimated with Cramer-Rao lower bounds <20%; and 2) calculation and comparison of the weighted means of metabolites' concentrations.

RESULTS: The main finding observed was a higher total *N*-acetyl aspartate concentration in superagers than in age-matched controls using both approaches ($P = .02$ and $P = .03$ for the weighted means), reflecting a positive association of total *N*-acetyl aspartate with higher cognitive performance.

CONCLUSIONS: ^{1}H-MR spectroscopy emerges as a promising technique to unravel neurochemical mechanisms related to cognitive aging in vivo and providing a brain metabolic signature in superagers. This may contribute to monitoring future interventional therapies to avoid or postpone the pathologic processes of aging.

ABBREVIATIONS: CRLB = Cramer-Rao lower bounds; Glu = glutamate; GCP = glycerophosphocholine; NAAG = *N*-acetyl aspartylglutamate; PCho = phosphocholine; PCr = phosphocreatine

Multifactorial neurobiologic mechanisms appear to underlie the complex phenomenon of superior cognitive performance in older adults.[1] Subjects exhibiting this outstanding phenotype are newly described as "superagers"[2] and have been studied by imaging, through structural[3] and functional MR imaging.[4] To date, it is known that superagers show selective cortical preservation involving regions of the default mode and salience networks, which also exhibit strong functional connectivity.[5] There is a paucity of data, in particular generated by ^{1}H-MRS, related to the metabolic profile of the brains of superagers.[6]

Previous studies have reported the correlation between ^{1}H-MR spectroscopy parameters of metabolite concentration with measures of intelligence,[7-9] affect,[10] creativity,[11] and personality[12] in cohorts of healthy human individuals, mostly younger adults. Such findings suggest that neurometabolites may be involved in healthy brain aging trajectories, such as those observed among superagers. Therefore, ^{1}H-MR spectroscopy, which noninvasively probes several brain metabolites, can be used to provide information on

Received November 3, 2020; accepted after revision May 28, 2021.

From the Departments of Radiology and Oncology (L.L.d.G., C.d.C.L.) and Neurology (A.S.-N., N.C.M., M.S.Y., R.N.), and Division and Laboratory of Nuclear Medicine (A.M.C., C.A.B.), Department of Radiology and Oncology, Hospital das Clinicas da Faculdade Medicina da Universidade de Sao Paulo, Sao Paulo, Brazil; The National Hospital of Neurology and Neurosurgery (L.L.d.G., M.W.-A., S.B.), University College London, London, UK; and Department of Biostatistics, Institute of Biosciences (M.H.T.), Universidade Estadual Paulista, Botucatu, Sao Paulo, Brazil.

L.L. de Goday and A. Studart-Neto share co-first authorship.

S. Bidas and C. da Costa Leite share co-senior authorship.

This work was funded by Fundação Amaro a Pesquisa do Estado de São Paulo (2.025.068).

Please address correspondence to Laiz Laura de Godoy, MD, The National Hospital of Neurology and Neurosurgery, University College London, London, United Kingdom, Queen Square, Holborn, London WC1N 3G, UK; e-mail: laizlgodoy@gmail.com; @sbisdas

Indicates open access to non-subscribers at www.ajnr.org

Indicates article with online supplemental data.

http://dx.doi.org/10.3174/ajnr.A7262

biochemical pathways associated with the cognitive status of the aging brain.[13]

Physiologic aging changes involve specific cellular mechanisms, such as bioenergetics, oxidative stress, inflammation, cell membrane turnover, and endogenous neuroprotection revealed by neurochemicals in ^{1}H-MR spectroscopy.[14] Overall, the aging brain shows a reduced concentration of NAA and glutamate (Glu) and an increased concentration of choline (Cho) and myo-inositol (mIns).[6] Few studies showed a positive correlation between the NAA concentration and better memory performance in healthy older adults.[6] Nevertheless, there are no studies to determine whether these age-related metabolite changes correlate with neuropsychological performance in superagers using age-matched controls for comparison.

^{1}H-MR spectroscopy under standardized conditions is necessary to obtain an accurate representation of the metabolic profile in vivo. First, the VOI must be placed in the least inhomogeneous area of gray or white matter. A high field strength (at least 3T) is needed to achieve better spectral resolution and a higher signal-to-noise ratio for metabolites present in tissue at a much lower concentration than in water or those affected by J-coupling.[15] Metabolite concentrations as relative ratios of creatine (Cr) should be avoided in older adults[16] because creatine seems to vary in the aging brain.[17] Finally, optimal shimming methods and implementation of post hoc correction based on tissue and CSF segmentation within the VOI are mandatory.[18]

In the present study, we sought to investigate any relationship between brain metabolite concentrations obtained by ^{1}H-MR spectroscopy with the late-life cognitive performance in a selected population of superagers and age-matched controls. We hypothesized that there is a different neurochemical signature between these 2 subject groups. Our results may be useful to address the resilience process of aging that underlies the superager's profile.

MATERIALS AND METHODS

Selection of Participants

Initially, 55 participants (Online Supplemental Data) were screened from different centers in the city of Sao Paulo, Brazil, including the outpatient clinic of the Geriatrics Department of Hospital das Clinicas da Faculdade de Medicina da Universidade de Sao Paulo; the Open University Program for Senior Citizens at the School of Arts, Sciences and Humanities Universidade de Sao Paulo; and the Development Center for the Promotion of Healthy Aging. We also screened community elderly volunteers through social media and newspaper campaigns. Informed consent was obtained from each participant, and the research project was approved by the Ethics Committee of the University of Sao Paulo (No. 62047616.0.0000.0068). The study was designed and conducted according to the Declaration of Helsinki.

The inclusion criteria for the participants were the following: 1) 80 years of age or older; 2) education ≥4 years; 3) Mini-Mental State Examination findings normal for their education status;[19,20] 4) Functional Activity Questionnaire score ≤ 4;[21] 5) Clinical Dementia Rating score equal to zero; and 6) the 15-question version of the Geriatric Depression Scale result of ≤5.

The exclusion criteria included the following: 1) diagnosis of dementia or mild cognitive impairment according to the criteria of the National Institute on Aging and Alzheimer's Association;[22,23] 2) diagnosis of a major psychiatric disorder by the *Diagnostic and Statistical Manual of Mental Disorders*, Fifth Edition; 3) a history of alcohol or psychoactive drug abuse; 4) current or previous diagnosis of diseases of the CNS (ie, stroke or seizure); 5) the presence of structural lesions in the CNS at image examination that could distort the brain parenchyma (ie, tumor or brain malformation); and 6) visual and/or auditory limitations that impair the performance of cognitive tests.

Neurocognitive Screening

The first assessment consisted of a semi-structured interview with the collection of sociodemographic data; cognitive assessment using the Mini-Mental State Examination, the Montreal Cognitive Assessment, and the Brief Cognitive Screening Battery;[24] screening for depressive symptoms and anxiety using the Geriatric Depression Scale-15 and the Geriatric Anxiety Inventory, respectively; and a functional assessment with the Functional Activity Questionnaire score and the Clinical Dementia Rating.

Subsequently, the subjects who met the inclusion criteria underwent neuropsychological tests. The tests included Digit Span Forward and Backward, Trail-Making Tests A and B, category (animals) and letter verbal fluency tests, Rey-Osterrieth Complex Figure (copy and delayed recall), Logical Memory of the Wechsler Memory Scale, Rey Auditory Verbal Learning Test, the 60-item version of the Boston Naming Test, and the estimated intelligence quotient, which was measured with the Wechsler Adult Intelligence Scale, Third Edition. Those who performed equal or less than −1.5 SDs from average normative values adjusted by age and education for any cognitive test aforementioned were excluded.

Healthy Older Adults Grouping

Participants were separated into 2 groups: namely superagers and age-matched controls. Superagers were defined as the participants who presented a delayed recall score (30 minutes) of the Rey Auditory Verbal Learning Test, a measure of episodic memory, equal to or greater than average normative values for individuals 50–60 years of age (≥9 words), according to the criteria established by the Northwestern SuperAging Research Program.[25] In addition, to fulfill this superager definition, they had to perform within or above 1 SD of the average range for their age and demographics for cognitive function in the nonmemory domains tests, including the Digit Span Forward and Backward, the Boston Naming Test-60, Trail-Making Tests A and B, the Rey-Osterrieth Complex Figure, and category (animals) and letter verbal fluency, according to the published normative values.[26,27] The age-matched controls performed within 1 SD of the average range for their age and demographics in memory and nonmemory domains, which means that they were average older adults according to their cognitive status.

MR Imaging

All MR imaging studies were performed on a 3T Signa PET/MR scanner (GE Healthcare) using a multichannel receiver (8HRBRAIN) radiofrequency coil. First, 3D volumetric T1-weighted images were acquired (TR = 7.7 ms; TE = 3.1 ms; TI = 600ms; in-plane resolution = 0.5 × 0.5 mm;^{2} section thickness =

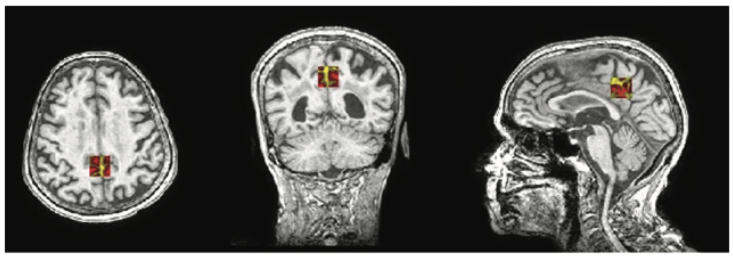

FIG 1. Voxel placement for ^{1}H-MR spectroscopy on the posterior cingulate cortex. CSF (yellow) and gray and white matter (red).

1 mm, isotropic) and were used for ^{1}H-MR spectroscopy voxel placement and to enable subsequent voxel segmentation to address the partial volume averaging. ^{1}H-MR spectroscopy data were acquired with a single-voxel point-resolved spectroscopy sequence, with a bandwidth of 5000 Hz. The standardized VOI measuring 20 × 20 × 20 mm^3 was always positioned on the posterior cingulate cortex as shown in Fig 1. ^{1}H-MR spectroscopy preacquisition adjustments included high-order shimming (automatic and manual) within the selected region and optimization of water suppression. Water-suppressed spectra were then acquired with TE = 35ms; TR = 1500ms; 4096 complex points; and 128 transients. A reference spectrum without water suppression was also obtained.

Data Analysis

All spectroscopic data were analyzed using LCModel (Version 6.3-1; http://www.lcmodel.com/).[28] Model spectra of 18 metabolites were included in the basis data set together with model spectra for macromolecules and lipids.[29] Metabolite levels were estimated using internal water as a reference. A typical value for tissue water content in the gray matter of 43,300 mM was applied.[30] The parameter was adjusted using T2 ~ 80 ms for the major tissue water component, as previously reported.[31] Metabolite levels were then corrected for partial volume of CSF in the ^{1}H-MR spectroscopy VOI using the following correction factor (CSFcor), CSFcor = 1.0/(1.0-CSF fraction). The CSF fraction was calculated according to standard practice.[32] Briefly, the steps were the following: 1) registration of the ^{1}H-MR spectroscopy VOI to 3D T1-weighted images; 2) segmentation of the 3D T1-weighted volume using the SPM 8 software (http://www.fil.ion.ucl.ac.uk/spm/software/spm12);[33] and 3) use of segmentation results to determine the brain tissue and CSF fractions in the ^{1}H-MR spectroscopy VOI.

Quality control of ^{1}H-MR spectroscopy spectra was performed before the inclusion of LCModel results for further analysis. We used the following criteria: signal-to-noise ratio > 12 (SNR obtained from LCModel analysis and defined as the maximum in a spectrum minus baseline over the Analysis Window to twice the root-mean-square of Residuals), and linewidths at full width at half maximum of 10 Hz (full width at half maximum obtained from LCModel analysis). The cutoff values for SNR and full width at half maximum were established experimentally as conservative thresholds to provide adequate quantitative assessment and consistent data quality across the 2 groups.[34]

Statistical Analysis

For metabolite concentrations, only those estimated values with relative Cramer-Rao lower bounds (CRLB) <20% were retained in the statistical analysis. We also used an alternative approach based on the "weighted mean method."[14]

Descriptive statistics including mean, SD, standard error, median, and quartiles were generated for all study variables and groups. Distribution normality of the variables was assessed using the Shapiro-Wilks test. The means and medians among groups were compared using the 2-sided *t* test for independent samples and/or the Mann-Whitney *U* test according to the normality assessment at $P < .05$. The comparison of means between groups was also performed using the weighted *t* test (weighted linear model) at $P < .05$.

For the weighted mean approach, the weights (Wi) for each metabolite estimate were calculated as the following equation:

$$w_i = \frac{1}{[C_i(\frac{R_i}{100})]^2},$$

where C_i is the estimated concentration of a metabolite, and R_i, the corresponding CRLB (%) measure. When the reliability is very low, CRLB% > 80% in the LCModel, the weight was defined as zero.

Then the weighted mean (*wM*) and weighted SD (*wSD*) were defined as

$$wM = \frac{\sum_{i=1}^{N} w_i c_i}{\sum_{i=1}^{N} w_i},$$

and

$$wSD = \sqrt{\frac{\sum_{i=1}^{N} w_i (C_i - wM)^2}{\sum_{i=1}^{N} w_i}},$$

where *i* is the measurement index and *N* is the number of measurements.

Qualitative Examination

In addition, a qualitative examination was performed on the basis of visual comparison of the spectral patterns shown by averaging spectra for each group (Fig 2). The difference spectrum was also calculated to highlight any differences among groups. The averaged spectra were calculated following normalization and spectral registration/alignment of individual within-group spectra using the FID-A tool (Matlab; MathWorks).[35]

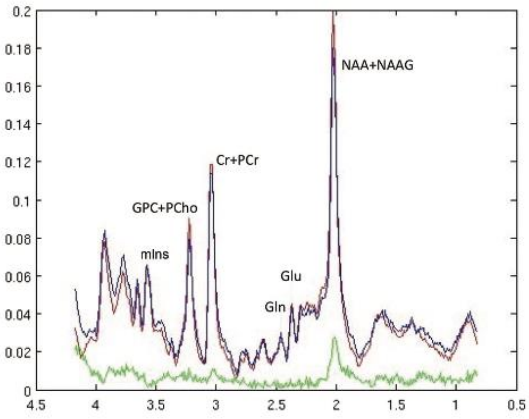

FIG 2. Averaged spectra for superagers (red), age-matched controls (blue), and the difference between groups (green). The most prominent difference is for NAA+NAAG (2.02 ppm), and there is a small difference for total Cr (3.03 ppm) and mIns (~3.56 ppm) metabolites.

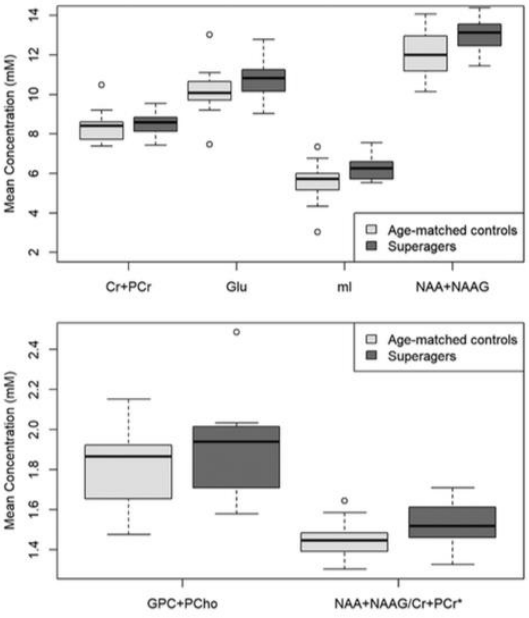

FIG 3. Boxplots showing metabolite concentration differences between superagers and age-matched controls. NAA+NAAG was statistically significantly more elevated in the posterior cingulate cortex of superagers than in age-matched controls ($P = .02$), and mIns tended to be higher in superagers ($P = .06$). Cr+PCr, Glu, GCP+PCho, and NAA+NAAG/Cr+PCr were not statistically significantly different across groups. The *asterisk* means do not consider the unit millimolar (mM) for the ratio NAA+NAAG/Cr+PCr.

RESULTS

Demographics and Neuropsychological Performance of Participants

Fourteen superagers and 15 age-matched controls were assessed through ^{1}H-MR spectroscopy, but 2 superagers and 2 age-matched controls were excluded due to a low SNR. Twelve superagers and 13 age-matched controls were included in the statistical analyses (Online Supplemental Data). On the basis of the selection criteria, superagers and age-matched controls did not differ in terms of age, education, or sex distribution (Online Supplemental Data). Superagers had statistically significantly better performance compared with age-matched controls in the Montreal Cognitive Assessment and some episodic memory tests (delayed recall of the Brief Cognitive Screening Battery, delayed recall of the Rey Auditory Verbal Learning Test, and delayed recall of the Logical Memory II). See the Online Supplemental Data for demographic and neuropsychological testing information.

^{1}H-MR spectroscopy

The location and size of the standardized voxel used for ^{1}H-MR spectroscopy are shown in Fig 1. Averaged spectra illustrate the spectral quality consistently obtained in the posterior cingulate cortex (Fig 2). On average, the SNR in the superagers spectra was 22.7 (SD, 3.8) and 19.8 (SD, 4.2) in controls. In the superagers, cortex linewidths full width at half maximum were 5.22 (SD, 0.64) Hz compared with 5.09 (SD, 0.77) Hz in the age-matched controls. Of 18 metabolites, 9 had CRLB% $<$ 20% (a frequently used inclusion criterion indicating acceptable fitting reliability; Online Supplemental Data). Four of them were sums of metabolites, including creatine+phosphocreatine (Cr+PCr); glycerophosphocholine+phosphocholine (GCP+PCho); glutamate+glutamine (Glu+Gln) and *N*- acetyl aspartate+*N*-acetylaspartyl glutamate (NAA+NAAG).

The results from the LCModel analysis were further processed using 2 approaches as aforementioned. First, only the concentrations of metabolites estimated with CRLB% $<$ 20% were considered for statistical analysis and comparisons; in the second, weighted means of the metabolite concentrations with CRLB% $<$ 20% were calculated and used to compare the 2 groups. The motivation for the second approach was to reflect the variable accuracy of fitted concentrations, providing rigor to the former findings. Superagers presented with statistically significantly higher NAA+NAAG concentrations than age-matched controls in both methods ($P = .02$ and $P = .03$ for the weighted means). However, the ratio NAA+NAAG/Cr+PCr did not reach statistical significance ($P = .06$) (Fig 3 and Online Supplemental Data).

mIns tended to be more increased in superagers than in average-age controls when considering metabolite concentration ($P = .06$), but it was not statistically significant when analyzing the weighted mean ($P = .09$). The remaining metabolites quantified reliably, including glycerophosphocholine+phosphocholine (GCP+PCho), Glu, and total creatine (PCr + Cr), did not demonstrate statistically significant differences between groups for both methods of measurement analysis (Fig 3 and Online Supplemental Data).

Tissue Composition

Superagers and age-matched controls did not differ significantly in the means of CSF and gray matter components in the VOIs; however, the groups showed statistically significant differences in the white matter content of the VOI composition, greater in superagers ($P = .04$) (Online Supplemental Data).

DISCUSSION

Our study highlighted and compared the metabolic differences in the posterior cingulate cortex of superagers and age-matched controls to find associations between superior memory performance and neurometabolites detected by ^{1}H-MR spectroscopy. We evaluated cognitive-related differences independent of age showing higher levels of total NAA (NAA+NAAG) in superagers using 2 different methods of analysis, suggesting a positive association of total NAA with higher cognitive function.

Although some studies have investigated cognitive-related metabolic changes in the normal aging brain,[6,36-41] to our knowledge, this is the first examination of metabolite concentrations in superagers. Our cohorts were made up of subjects older than 80 years of age because the concept of superior cognition as an index of resilience and resistance becomes more critical with age,[42] and subjects between 60 and 80 years of age may be biased to obtain meaningful assertions about "youthful" memory performance.[43,44] Furthermore, the reported literature of this age category is still limited.

We focused on the posterior cingulate cortex because it is one of the primary brain regions to display volume loss and reduced functional integrity during healthy aging and in neurodegenerative disorders.[45,46] Compared with the hippocampal formation, the ^{1}H-MR spectroscopy in the posterior cingulate cortex shows better homogenization of the magnetic field and fewer artifacts, providing more reliable and reproducible results.[47] The observed differences in neurochemical concentrations in this region appeared to be not noticeably susceptible to differences in the VOI composition between the 2 groups. Even though there was a statistically significant difference in the white matter fraction (superagers = 0.15; age-matched controls = 0.12), the results of the VOI analysis of the posterior cingulate cortex were predominantly driven by the gray matter fraction (superagers = 0.65; age-matched controls = 0.64) (Online Supplemental Data). Moreover, the effect of the CSF content on metabolite concentration was considered during quantification, and no substantial differences were detected in the total tissue fraction content.

Total NAA is the sum of NAA and NAAG. The separation between NAA and NAAG using the 3T ^{1}H-MR spectroscopy point-resolved spectroscopy sequence is inherently inaccurate; however, the sum of these metabolites can be estimated with good accuracy. NAA is a marker of neuronal and axonal function[38] and may be implicated in mitochondrial activity, representing a potential source of neuronal metabolic efficiency.[48] NAA can also be involved in myelin synthesis and maintenance.[49]

Previous findings in young adults have demonstrated that NAA levels are strongly associated with measures of intelligence,[7-9] creativity,[11] and, more recently, emotional constructs such as agency and flexibility.[50] Superagers, by definition, have superior episodic memory performance, which is an important component of intelligence, according to more recent theoretic models.[51] Therefore, our results support the relevance of the NAA levels in surrogate biomarkers of cognitive performance. Further studies are still necessary to investigate whether superagers may score higher on measures of creativity, emotion, and personality and whether such characteristics can be associated with the neurometabolic markers.

There is an agreement void in the literature regarding NAA levels in the normal-aging brain; however, studies using state-of-the-art single-voxel ^{1}H-MR spectroscopy showed an overall reduction in NAA,[52-56] notably in the frontal lobes and hippocampus.[6] Whole-brain ^{1}H-MR spectroscopy studies also found decreased NAA concentrations with aging.[57,58] In line with the literature, our age-matched controls presented with an expected reduction in the NAA concentration, further explaining some divergences among the previous aging studies in which the cognition status was not taken into account.

Even though different cognitive tasks and different VOIs were applied reporting cognitive-related metabolic changes in normal aging, our results in superagers are broadly in agreement with previous studies,[36-41] which have shown a consistent positive association between NAA levels and cognitive performance. The previous studies have demonstrated higher NAA concentrations associated with improved performance on executive function tasks, digit-span tasks, composite processing speeds, memory tasks, and psychomotor processing speeds, supporting our findings in superagers.

Because gray matter loss is a component of aging,[59] the reduction in NAA may be due to neuronal death or shrinkage.[60] The age-related reduction in synaptic density can also explain the decline in NAA concentration and underlie cognitive changes in older adults.[61] It is also known that levels of NAA are reduced in neurodegenerative diseases[62,63] such as Alzheimer disease, and its reduction has been associated with increased amyloid-β markers in normal aging[64] and in subjects with mild cognitive impairment.[65] Thus, ^{1}H-MR spectroscopy can be a noninvasive tool in vivo to diagnose, prognose, and monitor neurodegenerative disorders.

NAAG, a product of NAA, is a neurotransmitter that might be part of a compensatory neuroprotective mechanism through its actions on the presynaptic group II metabotropic glutamate receptors.[66,67] Harris et al,[14] in 2014, showed significantly higher NAAG in both the hippocampus and cortex of older animals, suggesting a protective response to the constitutively elevated glucose in aged brains. Moreover, NAAG has been shown to protect neurons in vitro from cell death after exposure to high glucose,[68,69] a metabolite that seems to play a key role in dementia pathology.[70]

In a previous study reporting cognitive-related metabolic changes in healthy older adults, Kochunov et al,[39] in 2010, showed a positive relationship between higher Cr and Cho and better memory performance. Another study demonstrated a negative association between higher Cho/Cr and Cho/mIns concentrations and a composite score of global cognition.[41] Our investigation did not find any differences in total Cho (GCP+PCho) in superagers compared with age-matched controls. Cho concentration seems to be elevated with age independent of cognitive status, notably in the posterior cingulate cortex and centrum semiovale,[17,53,71] reflecting, most likely, increased cell membrane turnover and breakdown.[14,56]

Our results suggest a lack of association between cognitive performance and the concentration of total Cr demonstrated in normal aging.[36] In addition, when considering total Cr as a denominator for the relative NAA+NAAG concentration (NAA+NAAG/Cr+PCr), we could not detect statistically significant differences between superagers and age-matched controls,

supporting previous findings that Cr changes are inconsistently associated with age.[6] On the basis of this inconsistent concentration pattern, Cr must be avoided to determine metabolite ratios in elderly samples and can be misleading when considered as a biomarker in this population.[16,36]

Our analysis suggested a trend toward increased mIns in superagers compared with the age-matched controls. mIns has been described as a marker of glial proliferation.[72,73] Nevertheless, this is questionable because brain tissue histopathology studies have not shown a statistically significant relationship between astrogliosis and mIns.[74] Ultimately, mIns has been proposed to function as an osmolyte in the brain and is potentially implicated in brain cell signaling.[75,76]

Glu is a neurotransmitter involved in cognition, learning, and memory.[56,77] Previous studies in dementia showed decreased Glu levels in mild cognitive impairment and notably in Alzheimer disease compared with healthy older adults.[78,79] Other studies have shown Glu reduction with age.[53,80] Among healthy older adults, when controlling for age, the literature lacks Glu examination for cognitive performance, and our study did not find differences in Glu concentration between the 2 groups. Nonetheless, more studies are still necessary to characterize the Glu role in cognition among the healthy elderly population.

The main strengths of our study were the use of a detailed and validated neuropsychological protocol to stratify older adults (older than 80 years of age) into superagers and age-matched controls and the implementation of standardized ^{1}H-MR spectroscopy acquisition.[17] Second, the VOI standardization and placement in the posterior cingulate cortex contribute to the generation of robust results that allow them to be easily validated in another setting. Finally, the implemented postprocessing methods, including measures of spectra quality and tissue/CSF segmentation to address the partial volume averaging in the ^{1}H-MR spectroscopy measurements, enhanced the quality and reproducibility of our results.[81]

Nevertheless, this study also presents some weaknesses. The published data concerning the prevalence of superagers in the global population are still insufficient[82] and did not allow us to undertake a power sample analysis before study conduction. In previous studies using the same inclusion criteria, the sample size of superagers varied from 12[2] to 56.[83] The examined metabolite concentrations were limited to those sampled in the posterior cingulate cortex; however, metabolite concentrations differ among distinct portions of the brain and between gray and white matter,[84] possibly having an unpredictable impact on normal aging and the superagers' metabolic signatures. Also, no inferences regarding the impact of aging on several metabolite levels could be drawn. Future studies with whole-brain ^{1}H-MR spectroscopy and control groups with younger volunteers would be useful to understand better metabolic profile changes during aging in different brain regions.

CONCLUSIONS

The present single-voxel ^{1}H-MR spectroscopy study provides in vivo evidence that superior memory performance in late life is positively associated with total NAA in the posterior cingulate cortex. These findings indicate that higher total NAA can contribute to the resilience process of the conventional pathways of aging present in superagers. Expanding on the current results, future evidence accumulation will probably qualify ^{1}H-MR spectroscopy as a diagnostic means for the quantification of neurochemical biomarkers in the aging population and as a prognostic tool including monitoring interventional therapies to preserve or enhance cognition in later life.

ACKNOWLEDGMENTS

We thank the participants and their families for their involvement and diligence and Hospital das Clinicas da Faculdade de Medicina da Universidade de Sao Paulo and The National Hospital of Neurology and Neurosurgery, University College London. We also thank Mrs Camila de Godoi Carneiro, MSc, for her technical support with data collection and anonymization, as well as data transfer across Institutions.

Disclosures: Marzena Wylezinska-Arridge—*UNRELATED*: *Employment*: National Hospital for Neurology and Neurosurgery. Carlos Buchpiguel—*RELATED*: *Grant*: Fundação Amaro a Pesquisa do Estado de São Paulo, *Comments*: Official Governamental Research Agency of São Paulo.* Ricardo Nitrini—*UNRELATED*: *Employment*: University of São Paulo Medical School; *Grants/Grants Pending*: Alzheimer's Association, Fundação Amaro a Pesquisa do Estado de São Paulo*; *Payment for Lectures Including Service on Speakers Bureaus*: One meeting prepared by Biogen. *Money paid to the institution.

REFERENCES

1. de Godoy LL, Alves CA, Saavedra JS, et al. **Understanding brain resilience in superagers: a systematic review.** *Neuroradiology* 2021;63:663–83 CrossRef Medline
2. Harrison TM, Weintraub S, Mesulam MM, et al. **Superior memory and higher cortical volumes in unusually successful cognitive aging.** *J Int Neuropsychol Soc* 2012;18:1081–85 CrossRef Medline
3. Gefen T, Peterson M, Papastefan ST, et al. **Morphometric and histologic substrates of cingulate integrity in elders with exceptional memory capacity.** *J Neurosci* 2015;35:1781–91 CrossRef Medline
4. Wang X, Ren P, Baran TM, et al. Alzheimer's Disease Neuroimaging Initiative. **Longitudinal functional brain mapping in supernormals.** *Cereb Cortex* 2019;29:242–52 CrossRef Medline
5. Zhang J, Andreano JM, Dickerson BC, et al. **Stronger functional connectivity in the default mode and salience networks is associated with youthful memory in superaging.** *Cereb Cortex* 2020;30:72–84 CrossRef Medline
6. Cleeland C, Pipingas A, Scholey A, et al. **Neurochemical changes in the aging brain: a systematic review.** *Neurosci Biobehav Rev* 2019;98:306–19 CrossRef Medline
7. Jung RE, Gasparovic C, Chavez RS, et al. **Imaging intelligence with proton magnetic resonance spectroscopy.** *Intelligence* 2009;37:192–98 CrossRef Medline
8. Jung RE, Yeo RA, Chiulli SJ, et al. **Myths of neuropsychology: intelligence, neurometabolism, and cognitive ability.** *Clin Neuropsychol* 2000;14:535–45 CrossRef Medline
9. Jung RE, Brooks WM, Yeo RA, et al. **Biochemical markers of intelligence: a proton MR spectroscopy study of normal human brain.** *Proc Bio Sci* 1999;266:1375–79 CrossRef Medline
10. Jung RE, Yeo RA, Love TM, et al. **Biochemical markers of mood: a proton magnetic resonance spectroscopy study of normal human brain.** *Biol Psychiatry* 2002;51:224–29 CrossRef Medline
11. Jung RE, Gasparovic C, Chavez RS, et al. **Biochemical support for the "Threshold" theory of creativity: a magnetic resonance spectroscopy study.** *J Neurosci* 2009;29:5319–25 CrossRef Medline
12. Ryman SG, Gasparovic C, Bedrick EJ, et al. **Brain biochemistry and personality: a magnetic resonance spectroscopy study.** *PLoS One* 2011;6:e26758 CrossRef Medline

13. Lee MR, Denic A, Hinton DJ, et al. **Preclinical (1)H-MRS neurochemical profiling in neurological and psychiatric disorders.** *Bioanalysis* 2012;4:1787–804 CrossRef Medline
14. Harris JL, Yeh HW, Swerdlow RH, et al. **High-field proton magnetic resonance spectroscopy reveals metabolic effects of normal brain aging.** *Neurobiol Aging* 2014;35:1686–94 CrossRef Medline
15. Schmitt F, Grosu D, Mohr C, et al. **3 Tesla MRI: successful results with higher field strengths.** *Radiologe* 2004;44:31–47 CrossRef Medline
16. Jansen JF, Backes WH, Nicolay K, et al. **1H MR spectroscopy of the brain: absolute quantification of metabolites.** *Radiology* 2006;240:318–32 CrossRef Medline
17. Chiu PW, Mak HK, Yau KK, et al. **Metabolic changes in the anterior and posterior cingulate cortices of the normal aging brain: proton magnetic resonance spectroscopy study at 3T.** *Age (Dordr)* 2014;36:251–64 CrossRef Medline
18. Oz G, Alger JR, Barker PB, et al. MRS Consensus Group. **Clinical proton MR spectroscopy in central nervous system disorders.** *Radiology* 2014;270:658–79 CrossRef Medline
19. Folstein MF, Folstein SE, McHugh PR. **Mini-Mental State: a practical guide for grading the mental state of patients for the clinician.** *J Psych Res* 1975;12:189–98 CrossRef Medline
20. Brucki S, Nitrini R, Caramelli P, et al. **Suggestions for utilization of the mini-mental state examination in Brazil** [in Portuguese]. *Arq Neuropsiquiatr* 2003;61:777–81 CrossRef Medline
21. Pfeffer RI, Kurosaki TT, Harrah CH Jr, et al. **Measurement of functional activities in older adults in the community.** *J Gerontol* 1982;37:323–29 CrossRef Medline
22. McKhann GM, Knopman DS, Chertkow H, et al. **The diagnosis of dementia due to Alzheimer's disease: recommendations from the National Institute on Aging-Alzheimer's Association workgroups on diagnostic guidelines for Alzheimer's disease.** *Alzheimers Dement* 2011;7:263–69 CrossRef Medline
23. Albert MS, DeKosky ST, Dickson D, et al. **The diagnosis of mild cognitive impairment due to Alzheimer's disease: recommendations from the National Institute on Aging-Alzheimer's Association workgroups on diagnostic guidelines for Alzheimer's disease.** *Alzheimers Dement* 2011;7:270–79 CrossRef Medline
24. Nitrini R, Caramelli P, Porto CS, et al. **Brief cognitive battery in the diagnosis of mild Alzheimer's disease in subjects with medium and high levels of education.** *Dement Neuropsychol* 2007;1:32–36 CrossRef Medline
25. Rogalski EJ, Gefen T, Shi J, et al. **Youthful memory capacity in old brains: anatomic and genetic clues from the Northwestern SuperAging Project.** *J Cogn Neurosci* 2013;25:29–36 CrossRef Medline
26. Heaton RK, Miller SW, Taylor MJ, et al. Revised comprehensive norms for an expanded Halstead-Reitan Battery: Demographically Adjusted Neuropsychological Norms For African American and Caucasian adults. 2004. http://www4.parinc.com/Products/Product.aspx?ProductID=RCNAAC. Accessed September 10, 2020
27. Shirk SD, Mitchell MB, Shaughnessy LW, et al. **A web-based normative calculator for the Uniform Data Set (UDS) neuropsychological test battery.** *Alzheimers Res Ther* 2011;3:32 CrossRef Medline
28. Provencher SW. **Estimation of metabolite concentrations from localizedin vivo proton NMR spectra.** *Magn Reson Med* 1993;30:672–79 CrossRef Medline
29. Seeger U, Klose U, Mader I, et al. **Parameterized evaluation of macromolecules and lipids in proton MR spectroscopy of brain diseases.** *Magn Reson Med* 2003;49:19–28 CrossRef Medline
30. Kreis R, Ernst T, Ross BD. **Absolute quantitation of water and metabolites in the human brain, II: metabolite concentrations.** *J Magn Reson B* 1993;102:9–19 CrossRef
31. Ernst T, Kreis R, Ross BD. **Absolute quantitation of water and metabolites in the human brain, I: compartments and water.** *J Magn Reson B* 1993;102:1–8 CrossRef
32. Edden RA, Puts NA, Harris AD, et al. **Gannet: a batch-processing tool for the quantitative analysis of gamma-aminobutyric acid–edited MR spectroscopy spectra.** *J Magn Reson Imaging* 2014;40:1445–52 CrossRef Medline
33. Friston KJ, Holmes AP, Worsley KJ, et al. **Statistical parametric maps in functional imaging: a general linear approach.** *Hum Brain Mapp* 1994;2:189–210 CrossRef
34. Pedrosa de Barros N, Slotboom J. **Quality management in in vivo proton MRS.** *Anal Biochem* 2017;529:98–116 CrossRef Medline
35. Simpson R, Devenyi GA, Jezzard P, et al. **Advanced processing and simulation of MRS data using the FID appliance (FID-A): an open source, MATLAB-based toolkit.** *Magn Reson Med* 2017;77:23–33 CrossRef Medline
36. Charlton RA, McIntyre DJO, Howe FA, et al. **The relationship between white matter brain metabolites and cognition in normal aging: the GENIE study.** *Brain Res* 2007;1164:108–16 CrossRef Medline
37. Driscoll I, Hamilton DA, Petropoulos H, et al. **The aging hippocampus: cognitive, biochemical and structural findings.** *Cereb Cortex* 2003;13:1344–51 CrossRef Medline
38. Ross AJ, Sachdev PS ,Wen W, et al. **Cognitive correlates of 1H MRS measures in the healthy elderly brain.** *Brain Res Bull* 2005;66:9–16 CrossRef Medline
39. Kochunov P, Coyle T, Lancaster J, et al. **Processing speed is correlated with cerebral health markers in the frontal lobes as quantified by neuroimaging.** *Neuroimage* 2010;49:1190–99 CrossRef Medline
40. Erickson KI, Weinstein AM, Sutton BP, et al. **Beyond vascularization: aerobic fitness is associated with N-acetylaspartate and working memory.** *Brain Behav* 2012;2:32–41 CrossRef Medline
41. Gomar JJ, Gordon ML, Dickinson D, et al. **APOE genotype modulates proton magnetic resonance spectroscopy metabolites in the aging brain.** *Biol Psychiatry* 2014;75:686–92 CrossRef Medline
42. Rogalski EJ. **Don't forget: age is a relevant variable in defining SuperAgers.** *Alzheimers Dement (Amst)* 2019;11:560–61 CrossRef Medline
43. Nyberg L, Lövdén M, Riklund K, et al. **Memory aging and brain maintenance.** *Trends Cogn Sci* 2012;16:292–305 CrossRef Medline
44. Borelli WV, Carmona KC, Studart-Neto A, et al. **Operationalized definition of older adults with high cognitive performance.** *Dement Neuropsychol* 2018;12:221–27 CrossRef Medline
45. Minoshima S, Giordani B, Berent S, et al. **Metabolic reduction in the posterior cingulate cortex in very early Alzheimer's disease.** *Ann Neurol* 1997;42:85–94 CrossRef Medline
46. Lehmann M, Rohrer JD, Clarkson MJ, et al. **Reduced cortical thickness in the posterior cingulate gyrus is characteristic of both typical and atypical Alzheimer's disease.** *J Alzheimers Dis* 2010;20:587–98 CrossRef Medline
47. Park EJ, Lyra KP, Lee HW, et al. **Correlation between hippocampal volumes and proton magnetic resonance spectroscopy of the posterior cingulate gyrus and hippocampi in Alzheimer's disease.** *Dement Neuropsychol* 2010;4:109–13 CrossRef Medline
48. Scavuzzo CJ, Moulton CJ, Larsen RJ. **The use of magnetic resonance spectroscopy for assessing the effect of diet on cognition.** *Nutr Neurosci* 2018;21:1–15 CrossRef Medline
49. Chakraborty G, Mekala P, Yahya D, et al. **Intraneuronal N-acetylaspartate supplies acetyl groups for myelin lipid synthesis: evidence for myelin-associated aspartoacylase.** *J Neurochem* 2001;78:736–45 CrossRef Medline
50. White TL, Gonsalves MA, Cohen RA, et al. **The neurobiology of wellness: 1H-MRS correlates of agency, flexibility and neuroaffective reserves in healthy young adults.** *Neuroimage* 2021;225:117509 CrossRef Medline
51. Jewsbury PA, Bowden SC, Duff K. **The Cattell–Horn–Carroll Model of cognition for clinical assessment.** *J Psychoeduc Assess* 2017;35:547–67 CrossRef
52. Hädel S, Wirth C, Rapp M, et al. **Effects of age and sex on the concentrations of glutamate and glutamine in the human brain.** *J Magn Reson Imaging* 2013;38:1480–87 CrossRef Medline
53. Marjańska M, Riley McCarten J, Hodges J, et al. **Region-specific aging of the human brain as evidenced by neurochemical profiles measured noninvasively in the posterior cingulate cortex and the**

Supplementary Figure 1.

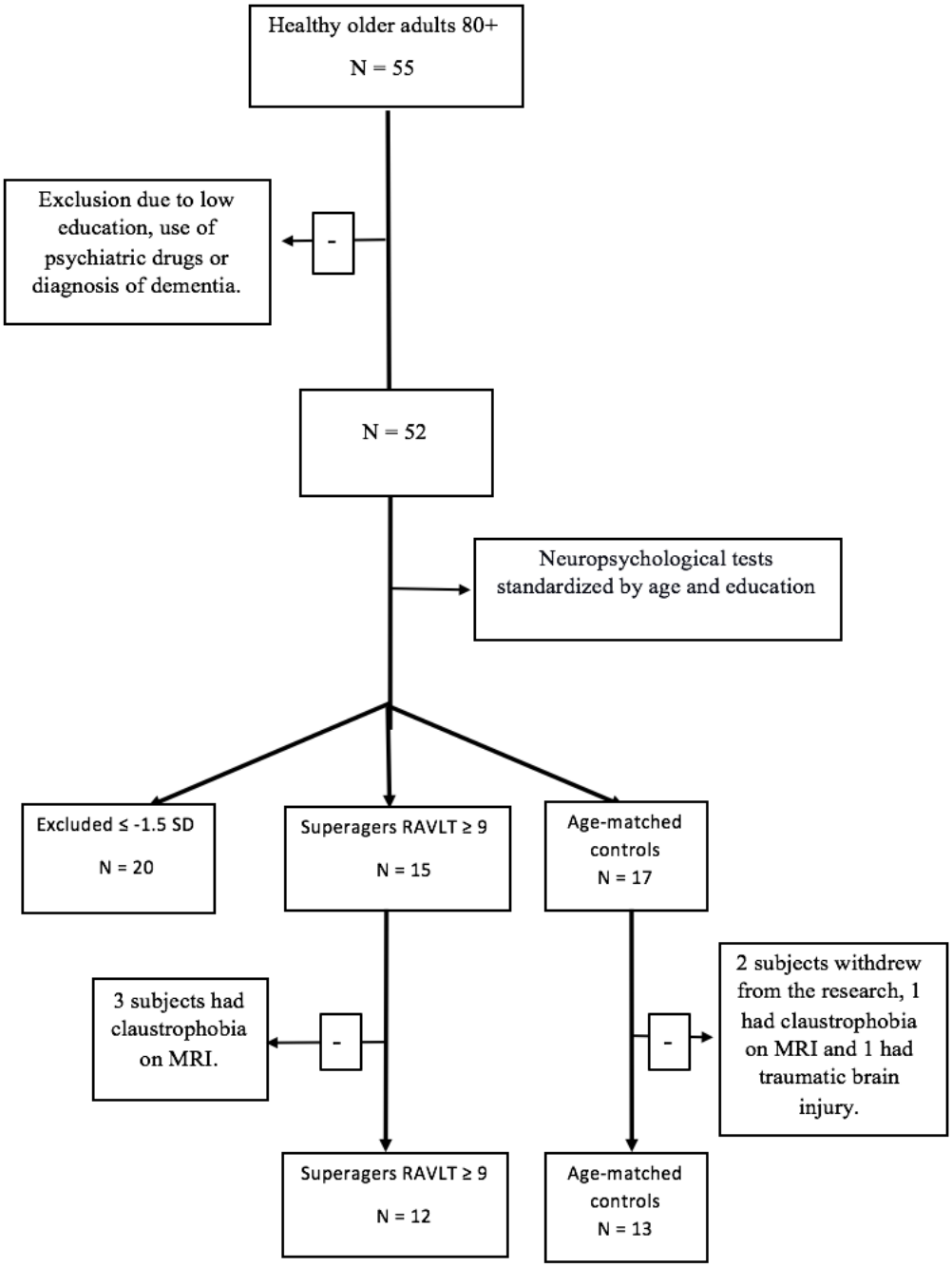

Supplementary Figure 1. Flowchart of participant selection and inclusion criteria for our cohort

Supplementary Table 1. Demographic information and neuropsychological test scores

	Age-matched controls (n = 13)		Superagers (n = 12)		p-value
	Mean (SD)	Median (IQR)	Mean (SD)	Median (IQR)	
Age (y)	84.38 (3.97)	84.00 (5.5)	83.42 (3.53)	82.00 (5.80)	0,54 [q]
Education (y)	14.54 (3.91)	16.00 (3.00)	15.92 (5.07)	17.50 (7.80)	0,27 [a]
Gender (%, male)	10 (76.90)		6 (50.00)		0,16 [b]
Psychiatric disorder (%)	1 (8.30)		1 (8.30)		0,76 [b]
Heart disease (%)	3 (25.00)		2 (16.70)		0,50 [b]
Hypothyroidism (%)	2 (16.70)		3 (25.00)		0,50 [b]
Dyslipidemia (%)	3 (25.00)		2 (16.70)		0,50 [b]
Diabetes mellitus (%)	2 (16.70)		3 (25.00)		0,50 [b]
Systemic arterial hypertension (%)	7 (58.30)		7 (58.30)		0,66 [b]
RAVLT Delay-Recall [c]	5.89 (1.52)	6.00 (2.00)	11.08 (1.44)	12.00 (2.80)	**< 0,001** [a]
MMSE [d]	28.38 (0.96)	28.00 (1.00)	28.92 (1.08)	29.00 (2.00)	0,27 [a]
MoCA [e]	23.54 (1.33)	24.00 (1.5)	26.50 (1.98)	27.00 (1.8)	**0,001** [a]
Delay-Recall BCSB [f]	7.0 (1.68)	7.00 (3.50)	8.58 (1v h80.16)	8.00 (2.00)	**0,019** [a]
Test Clock Drawing	9.46 (0.78)	10.00 (1.00)	9.00 (2.26)	10.00 (1.00)	0,98 [a]
Category Verbal Fluency (animals)	16.31 (4.23)	16.00 (5.50)	19.50 (6.38)	18.00 (7.80)	0,18 [a]
Letter Verbal Fluency (FAS)	40.69 (14.57)	34.00 (23.50)	45.75 (13.99)	43.00 (19.80)	0,32 [a]
Logical Memory II	18.77 (7.92)	17.00 (11.00)	28.75 (5.15)	27.50 (5.80)	**0,005** [q]
Rey Complex Figure (Copy)	32.89 (4.98)	34.00 (4.50)	35.67 (0.78)	36.00 (0.00)	0,07 [a]
Rey Complex Figure (Delay-Recall)	12.00 (4.76)	11.00 (8.80)	15.46 (5.63)	17.25 (8.00)	0,11 [a]
Trail Making A	48.54 (14.66)	47.00 (19.50)	49.17 (13.09)	51.00 (22.50)	0,98 [a]
Trail Making B	124.15 (51.40)	113.00 (66.50)	108.33 (39.64)	107.00 (65.80)	0,47 [a]
Forward Digit Span	7.77 (1.64)	8.00 (3.00)	9.25 (2.42)	9.00 (2.80)	0,11 [a]
Backward Digit Span	4.85 (2.11)	5.00 (3.00)	6.08 (1.24)	6.00 (2.00)	0,08 [a]
BNT- 60 [g]	54.92 (4.75)	56.00 (7.50)	56.83 (3.66)	58.00 (6.50)	0,29 [a]

Supplemental Table 1. Abbreviations: a. Mann-Whitney Test; **b.** Fisher's Exact Test; **c.** Rey Auditory Verbal Learning Test (RAVLT); **d.** Mini Mental State Examination (MMSE); **e.** Montreal Cognitive Assessment (MoCA); **f.** Brief Cognitive Screening Battery (BCSB); **g.** Boston Naming Test (BNT-60)

Supplementary Table 2. Metabolites' concentrations

	Average metabolites' concentrations			Weighted means of metabolites' concentrations		
	Posterior Cingulate Cortex					
	Superagers	Age-matched Controls	P	Superagers	Age-matched Controls	P
NAA+NAAG	13.06 (0.25)	12.05 (0.31)	**0.02**	12.87 (0.71)	12.09 (0.94)	**0.03**
NAA+NAAG/ Cr+PCr	1.53 (0.03)	1.45 (0.03)	0.06	1.50 (0.10)	1.45 (0.09)	0.69
mI	6.26 (0.18)	5.56 (0.30)	0.06	6.29 (0.62)	5.76 (0.90)	0.09
PCr	5.95 (0.16)	5.83 (0.33)	0.76	5.83 (0.58)	5.67 (0.91)	0.62
Cr+PCr	8.53 (0.17)	8.32 (0.23)	0.49	8.56 (0.55)	8.25 (0.78)	0.28
Gln	4.68 (0.35)	4.57 (0.34)	0.82	4.45 (0.10)	4.48 (1.21)	0.94
Glu	10.89 (0.30)	10.19 (0.35)	0.15	10.69 (0.96)	10.19 (1.14)	0.54
Glu+Gln	15.57 (0.60)	14.76 (0.57)	0.33	15.18 (1.81)	14.70 (1.92)	0.23
GPC+PCho	1.90 (0.07)	1.82 (0.05)	0.35	1.87 (0.23)	1.82 (0.19)	0.63
GSH	1.65 (0.12)	1.76 (0.11)	0.52	1.66 (0.38)	1.73 (0.37)	0.67
Tissue composition in the examined volume of interest						
GMf	0.65 (0.01)	0.64 (0.02)	0.85			
WMf	0.15 (0.01)	0.12 (0.01)	**0.04**			
CSFf	0.20 (0.02)	0.24 (0.02)	0.17			
Tissuef	0.80 (0.02)	0.76 (0.02)	0.20			

Supplemental table 2. Metabolite concentrations with CRLB < 20% are expressed in mM (millimols) for both analyses, namely the average metabolites' concentrations and their weighted means. The standard error of the means is displayed in brackets. The p-value for any significant differences for metabolite concentrations and weight is set at < 0.05

Abbreviations: NAA+NAAG, *N*- acetyl aspartate+N-acetylaspartyl glutamate; mI, Myo-inositol; PCr; phosphocreatine; Cr+PCr, Creatine+phosphocreatine; Gln, glutamine; Glu, Glutamate; Glu+Gln, Glutamate+Glutamine; GPC+PCho, Glyrecophosphocholine+phosphocholine; GSH, Glutathione. GMf, gray matter fraction; WMf, white matter fraction; CSFf, cerebrospinal fluid fraction; Tissuef, tissue fraction. The fractions are ratios of the volume taken up by GM, WM, CSF and tissue to the total volume of the ^{1}H-MRS VOI.

Supplementary Table 3 - Mean Weights. Posterior Cingulate Cortex

	Superagers	Age-matched Controls
NAA+NAAG	9.92	8.59
mI	15.77	14.54
PCr	2.05	2.06
Cr+PCr	24.50	23.93
Gln	2.05	1.90
Glu	2.80	2.55
Glu+Gln	1.58	1.53
GPC+PCho	216.55	214.36
GSH	14.66	12.76

Supplemental table 3. Mean weights calculated using the following equation to estimate the weight (w_i) of each metabolite: $w_i = \frac{1}{[C_i\,(\frac{R_i}{100})]^2}$

Abbreviations: NAA+NAAG, *N*- acetyl aspartate+N-acetylaspartyl glutamate; mI, Myo-inositol; PCr; phosphocreatine; Cr+PCr, Creatine+phosphocreatine; Gln, glutamine; Glu, Glutamate; Glu+Gln, Glutamate+Glutamine; GPC+PCho, Glycerophosphocholine+phosphocholine; GSH, Glutathione.

3.2 ARTIGO 2

Title: Phenotyping superagers by using resting-state functional magnetic resonance imaging

.

Running Title: *Phenotyping Superagers by rs-fMRI*

Authors:

Name	Orcid
Laiz L. de Godoy[a,b]	0000-0001-5956-5741
Adalberto Studart-Neto[c]	0000-0003-2260-5986
Demetrius Ribeiro de Paula[d]	0000-0003-0590-8694
Nathan Green[e]	0000-0003-2745-1736
Arjama Halder[f]	0000-0002-3195-9623
Paula Arantes[a]	0000-0001-6974-644X
Khallil Taverna Chaim[a]	0000-0002-5803-0099
Natália Cristina Moraes[c]	0000-0002-8439-6828
Mônica Sanches Yassuda[c]	0000-0002-9182-2450
Ricardo Nitrini[c]	0000-0002-5721-1525
Martin Dresler[d]	0000-0001-7441-3818
Claudia da Costa Leite[a]	0000-0002-1168-0780
Jasmina Panovska-Griffiths[g,h]	0000-0002-7720-1121
Andrea Soddu[i]	0000-0001-6833-745X
Sotirios Bisdas[b]	0000-0001-9930-5549

Institutions:

[a] Department of Radiology and Oncology, Hospital das Clinicas, Faculdade de Medicina FMUSP, Universidade de Sao Paulo, Sao Paulo, SP, Brazil.

[b] Lysholm Department of Neuroradiology, The National Hospital of Neurology and Neurosurgery, University College London, London, United Kingdom (UK).

[c] Department of Neurology, Hospital das Clinicas, Faculdade de Medicina FMUSP, Universidade de Sao Paulo, Sao Paulo, SP, Brazil.

[d] Donders Institute for Brain Cognition and Behavior, Radboud University Medical Centre, Nijmegen, The Netherlands.

[e] Department of Statistics, University College London, London, United Kingdom (UK).

[f] Department of Medical Biophysics, University of Western Ontario, London, ON, Canada.

[g] Big Data Institute, University of Oxford, Oxford, United Kingdom (UK).

[h] The Queen's College, University of Oxford, Oxford, United Kingdom (UK).

[I] Department of Physics and Astronomy, Western Institute for Neuroscience, University of Western Ontario, London, ON, Canada.

Correspondence to:
Laiz Laura de Godoy, MD.
Post-Doctoral Research Fellow.
Current affiliation: Department of Radiology, Perelman School of Medicine at the University of Pennsylvania, Philadelphia, PA, USA.
Tel. 215-662-6865
Email: laiz.godoy@pennmedicine.upenn.edu

Authors' Contributions:

Laiz Laura de Godoy: Conceptualization; Data curation; Investigation; Project administration; Writing - original draft; Writing - review & editing.

Adalberto Studart-Neto: Conceptualization; Data curation; Investigation; Writing - original draft.

Demetrius Ribeiro de Paula: Formal analysis; Methodology; Software; Writing - original draft.

Nathan Green: Formal analysis; Writing - original draft.

Arjama Halder: Software; Writing - review & editing.

Paula Arantes: Data curation; Writing - review & editing.

Khallil Taverna Chaim: Methodology; Software; Writing - original draft.

Natália Cristina Moraes: Data curation; Writing - review & editing.

Mônica Sanches Yassuda: Data curation; Writing - review & editing.

Ricardo Nitrini: Conceptualization; Data curation; Investigation.

Martin Dresler: Methodology; Writing - review & editing.

Claudia da Costa Leite: Conceptualization; Investigation; Supervision; Writing - review & editing.

Jasmina Panovska-Griffiths: Formal analysis; Methodology; Supervision; Writing - review & editing.

Andrea Soddu: Conceptualization; Investigation; Methodology; Software; Supervision; Writing - review & editing.

Sotirios Bisdas: Conceptualization; Investigation; Methodology; Supervision; Writing - review & editing.

MeSH Terms: Keywords: superagers; networks; rs-fMRI; aging; memory

ORIGINAL RESEARCH
FUNCTIONAL

Phenotyping Superagers Using Resting-State fMRI

LL. de Godoy, A. Studart-Neto, D.R. de Paula, N. Green, A. Halder, P. Arantes, K.T. Chaim, N.C. Moraes, M.S. Yassuda, R. Nitrini, M. Dresler, C. da Costa Leite, J. Panovska-Griffiths, A. Soddu, and S. Bisdas

ABSTRACT

BACKGROUND AND PURPOSE: Superagers are defined as older adults with episodic memory performance similar or superior to that in middle-aged adults. This study aimed to investigate the key differences in discriminative networks and their main nodes between superagers and cognitively average elderly controls. In addition, we sought to explore differences in sensitivity in detecting these functional activities across the networks at 3T and 7T MR imaging fields.

MATERIALS AND METHODS: Fifty-five subjects 80 years of age or older were screened using a detailed neuropsychological protocol, and 31 participants, comprising 14 superagers and 17 cognitively average elderly controls, were included for analysis. Participants underwent resting-state-fMRI at 3T and 7T MR imaging. A prediction classification algorithm using a penalized regression model on the measurements of the network was used to calculate the probabilities of a healthy older adult being a superager. Additionally, ORs quantified the influence of each node across preselected networks.

RESULTS: The key networks that differentiated superagers and elderly controls were the default mode, salience, and language networks. The most discriminative nodes (ORs $>$ 1) in superagers encompassed areas in the precuneus posterior cingulate cortex, prefrontal cortex, temporoparietal junction, temporal pole, extrastriate superior cortex, and insula. The prediction classification model for being a superager showed better performance using the 7T compared with 3T resting-state-fMRI data set.

CONCLUSIONS: Our findings suggest that the functional connectivity in the default mode, salience, and language networks can provide potential imaging biomarkers for predicting superagers. The 7T field holds promise for the most appropriate study setting to accurately detect the functional connectivity patterns in superagers.

ABBREVIATIONS: ASSET = array spatial sensitivity encoding technique; BOLD = blood oxygen level–dependent; DMN = default mode network; ECN-L = executive control network left; ECN-R = executive control network right; EN = elastic net; ICA = independent component analysis; IPAT = integrated parallel acquisition technique; rs-fMRI = resting-state fMRI; OLS = ordinary least squares; SN = salience network

Aging is an increasingly global phenomenon, usually accompanied by cognitive decline, with direct implications for the health care system and individuals' lives.[1] In this setting, subjects with superior memory performance in late life (80 years of age or older) stand out because they have a model capable of clarifying the brain mechanisms underlying cognitive resilience. These subjects have been identified as "superagers" in the literature.[2] To date, it is known that superagers show selective cortical preservation in particular regions of the default mode network (DMN) and salience network (SN), overlapped by stronger functional connectivity, highlighting possible key hubs for memory and cognition.[3-5] However, these studies included subjects from 60 years of age, which may be biased to obtain meaningful assertions about "youthful" memory performance in late life (80 years of age and older).[6]

Cognitive maintenance in older adults may reflect intrinsic functional integrity as a neurobiologic substrate.[7] fMRI can play an important role in detecting key brain hubs sustaining youthful cognition, thereby contributing to understanding the most resilient brain areas in superagers. Moreover, alterations in the brain functional connectome were previously reported to provide biomarkers for age-related cognitive decline and Alzheimer disease.[8]

Received July 28, 2022; accepted after revision February 19, 2023.

From the Departments of Radiology and Oncology (L.L.d.G., P.A., K.T.C., C.d.C.L.) and Neurology (A.S.-N., N.C.M., M.S.Y., R.N.), Hospital das Clinicas, Faculdade de Medicina da Universidade de Sao Paulo, Universidade de Sao Paulo, Sao Paulo, Brazil; Lysholm Department of Neuroradiology (L.L.d.G., S.B.), The National Hospital of Neurology and Neurosurgery, and Department of Statistics (N.G.), University College London, London, UK; Donders Institute for Brain Cognition and Behavior (D.R.d.P., M.D.), Radboud University Medical Centre, Nijmegen, the Netherlands; Departments of Medical Biophysics (A.H.), and Physics and Astronomy (A.S.), University of Western Ontario, London, Ontario, Canada; The Big Data Institute and the Pandemic Sciences Institute (J.P.-G.), and The Queen's College (J.P.-G.), University of Oxford, Oxford, UK.

Sotirios Bisdas, Andrea Soddu, and Jasmina Panovska-Griffiths contributed equally to this work.

Please address correspondence to Laiz Laura de Godoy, MD, Department of Radiology, Perelman School of Medicine at the University of Pennsylvania, 3400 Spruce St, Philadelphia, PA 19104; e-mail: laiz.godoy@pennmedicine.upenn.edu; @SBisdas

Indicates article with online supplemental data.

http://dx.doi.org/10.3174/ajnr.A7820

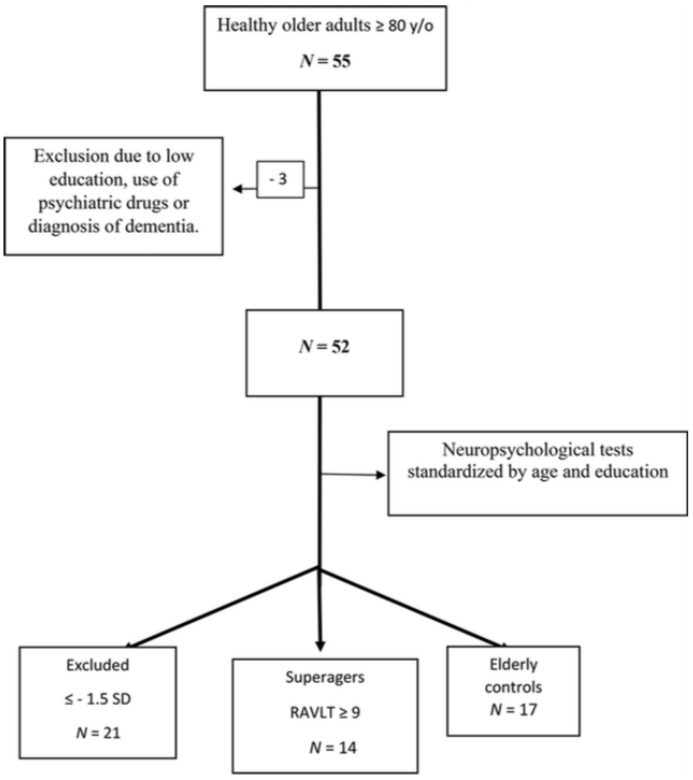

FIG 1. Flow chart of participant selection. RAVLT indicates the Rey Auditory Verbal Learning Test; y/o, years of age.

weighted echo-planar imaging sequence with the following parameters: TR = 2000 ms, TE = 30 ms, flip angle = 90°, FOV = 240 × 240, matrix = 80 × 80, section thickness = 3.6 mm (voxel size = 3 × 3 × 3.6 mm), number of slices = 36, gap = 0.4 mm, ASSET factor = 2.5. Although 208 volumes were acquired during 6 minutes 56 seconds, the first 4 volumes were discarded, so we had 204 volumes per subject.

The 7T MR imaging was performed after acquiring all the data on the 3T scanner and within 6 months after the clinical evaluation. We used a Magnetom 7T scanner (Siemens) with a 32-channel coil (Nova Medical). The 3D T1 image was acquired by the MP2RAGE technique with the following parameters: TR = 6000 ms, TE = 2.25 ms, flip angle = 4°/5°, TI = 800/2700 ms, integrated parallel acquisition technique (IPAT) = 3, FOV = 240 × 240, matrix = 320 × 320, and 256 slices, yielding an isotropic voxel size of 0.75 mm^3 during 9 minutes 36 seconds. rs-fMRI was acquired with a T2*-weighted EPI multiband sequence, provided by the Center for Magnetic Resonance Research, with the following parameters: TR = 1500 ms, TE = 24 ms, flip angle = 70°, FOV = 210 × 210, matrix = 120 × 120, section thickness = 1.75 mm (isotropic voxel size = 1.75 mm^3), number of slices = 81, no gap, multiband accel factor 3, IPAT = 2, and 250 volumes were acquired in 6 minutes 38 seconds.

During the rs-fMRI at 3T and 7T, participants were told to keep their eyes open while looking at a fixation cross. No cognitive tasks or tests were administered before the MR imaging session.

Brain Connectivity Analysis

rs-fMRI Preprocessing. The MR imaging DICOM files were entered into an automatic pipeline in GraphICA (https://www.brainet.ca/) (Online Supplemental Data).[20] Anatomic and functional images were kept in native space and preprocessed using FSL 6.03 (http://www.fmrib.ox.ac.uk/fsl).[21] Preprocessing steps of the T1-weighted anatomic images included bias field correction, brain extraction, tissue-type segmentation (CSF, gray matter, white matter), and subcortical segmentation. On the functional data, we performed skull stripping, motion correction, section-timing correction, spatial smoothing (ceiling of 1.5 × voxel size), independent component analysis (ICA)-based Automatic Removal Of Motion Artifacts, high-pass filtering of 100 seconds, and nuisance regression of white matter and CSF.

Extraction of the Functional Networks. Graphica performs ICA with dual regression implemented in FSL.[21] As a part of this process, a set of independent component maps were identified for each network, and dual regression was implemented to identify subject-specific spatial maps using 11 resting-state network masks: auditory, DMN, executive control network left (ECN-L), executive control network right (ECN-R), hippocampal, language, SN, sensorimotor, visual lateral, visual medial, and visual occipital.

Regional Parcellation. Each subject's T1-weighted image was automatically segmented with a pipeline implemented in FreeSurfer (Version 7.1.0; http://surfer.nmr.mgh.harvard.edu). Further parcellation was performed with Graphica using a gradient-weighted Markov Random Field Model procedure described in Schaefer et al.[22] The procedure yielded 832 parcellated brain regions, which were included as network nodes for further analyses.

Functional Network Construction and Thresholding. After we coregistered each of the functional resting-state networks to the subject, a mean *z* value was calculated by averaging the scalar map values of the voxel belonging to each one of the 832 ROIs. The resulting *z*-standardized correlation coefficients describe the loading of each nodal time course on the respective resting-state networks. To remove spurious or weak *z* values, for instance, due to noise, the loadings were thresholded with a data-driven mixture modeling approach at a single-subject level.[23]

Resting-state fMRI (rs-fMRI) focuses on the temporal characteristics and spatial organization of spontaneous fluctuations of the blood oxygen level–dependent (BOLD) signal and is powerful for characterizing brain organization and its abnormalities. Because the discrepancies between superagers and cognitively average elderly controls may be modest-but-important to detect early changes in brain function, using an ultra-high-field rs-fMRI with increased spatial and temporal resolution may allow study of more subtle disruption.[9] This is the first time that older adults with superior memory performance have been investigated at a 7T field.

In this study, we compared the differences in the resting-state functional connectivity between superagers and cognitively average elderly controls (elderly controls) in a range of neural networks with the aim of identifying the most discriminative networks and within-network nodes for predicting superagers. We additionally examined differences in the prediction probability of being a superager between the rs-fMRI data at 3T and 7T magnetic fields. We hypothesized that hub regions are critical to predicting youthful cognitive function in superagers, and the measurements of functional connectivity would be improved at a higher magnetic field.

MATERIALS AND METHODS

Selection of Participants

Initially, 55 participants were recruited from different centers in the city of Sao Paulo, Brazil, as detailed previously by de Godoy et al,[10] and the neuropsychological tests were performed at the Department of Neurology of Hospital das Clinicas (Medical School of the University of Sao Paulo). Informed consent was obtained from each participant and the research project was approved by the Ethics Committee of the University of Sao Paulo (#62047616.0.0000.0068). The study was designed and conducted according to the Declaration of Helsinki.

The inclusion criteria for the participants were the following: 1) 80 years of age and older; 2) education of ≥ 4 years; 3) Mini-Mental State Examination scores normal for the individuals' education;[11,12] 4) Functional Activity Questionnaire score of ≤ 4;[13] 5) Clinical Dementia Rating score equal to zero; and 6) a result of the 15-question version of the Geriatric Depression Scale of ≤5.

The exclusion criteria included the following: 1) a diagnosis of dementia or mild cognitive impairment according to the National Institute on Aging and Alzheimer's Association criteria;[14,15] 2) a diagnosis of a major psychiatric disorder by the *Diagnostic and Statistical Manual of Mental Disorders, Fifth Edition*; 3) a history of alcohol or psychoactive drug abuse; 4) current or previous diagnosis of diseases of the CNS (ie, stroke or seizure); 5) the presence of structural lesions in the CNS on imaging that could distort the brain parenchyma (ie, tumor or brain malformation); and 6) visual and/or auditory limitations that impair the performance of cognitive tests.

The flow charts of participant selection and the neuropsychological tests performed are shown in Fig 1 and the Online Supplemental Data, respectively.

Neurocognitive Screening

The first assessment consisted of a semistructured interview with the collection of sociodemographic data; cognitive assessment using the Mini-Mental State Examination, Montreal Cognitive Assessment, and the Brief Cognitive Screening Battery;[16] screening for depressive symptoms and anxiety using the Geriatric Depression Scale-15 and the Geriatric Anxiety Inventory, respectively; and functional assessment with the Functional Activity Questionnaire and Clinical Dementia Rating.

Subsequently, the subjects who met the inclusion criteria underwent neuropsychological tests. The tests included the Forward and Backward Digit Span, Trail-Making A and B, Verbal Fluency (animals) and Letter Verbal Fluency tests, Rey-Osterrieth Complex Figure (copy and delayed recall), Logical Memory of the Wechsler Memory Scale, Rey Auditory Verbal Learning Test, 60-item version of the Boston Naming Test, and Estimated Intelligence Quotient measured with the Wechsler Adult Intelligence Scale, Third Edition. Those who performed equal or less than −1.5 SDs from average normative values adjusted by age and education for any cognitive test aforementioned were excluded.

Healthy Older Adult Grouping

Participants were separated into 2 groups: superagers (n = 14; mean age, 82.93 [SD, 3.47] years) and cognitively average elderly controls (n = 17; mean age, 84.47 [SD, 4.29] years). Superagers were defined as the participants who presented with a delayed recall score (30 minutes) in the Rey Auditory Verbal Learning Test, used as a measure of episodic memory, equal to or greater than average normative values for individuals 50–60 years of age (≥9 words), according to the criteria established by the Northwestern SuperAging research program.[2] In addition, to conform with these criteria, they had to perform at or above 1 SD of the average for their age and demographics for cognitive function in the nonmemory domains tests, including Forward and Backward Digit Span, 60-item version of the Boston Naming Test, Trail-Making A, Trail-Making B, Rey-Osterrieth Complex Figure, and Verbal Fluency (animals) and Letter Verbal Fluency tests.[17,18] The cognitively average elderly controls performed in memory and nonmemory domains within 1 SD of the average range for their age and demographics, which means that they were average-performing older adults according to their cognitive status.

Imaging Data Acquisition

We acquired MR imaging data of 31 participants (14 superagers and 17 elderly controls) on a 3T scanner, whereas 21 of them (12 superagers and 9 elderly controls) were also imaged on a 7T scanner. The fewer subjects scanned at the 7T field were due to MR imaging safety concerns (eg, the presence of ferromagnetic aneurysm clips, pacemakers, and stents)[19] and the safety measures in place during the coronavirus disease 2019 (COVID-19) pandemic.

The 3T MR imaging session was scheduled <1 month after the clinical and neuropsychological assessments. We used a Signa PET/MR imaging 3T scanner (GE Healthcare) with a 32-channel head coil. An anatomic whole-brain 3D T1-weighted scan was acquired with the parameters as follows: TR = 8 ms, TE = 3.2 ms, flip angle = 80°, array spatial sensitivity encoding technique (ASSET) factor = 1.5, FOV = 240 × 240, matrix = 240 × 240, and 180 slices of 1 mm each yielding a voxel size = 1 × 1 × 1 mm during 5 minutes 16 seconds. rs-fMRI was acquired with a T2*-

Global Properties. Global properties include the number of found, missing, and extra regions. These properties were calculated on the basis of template masks created and separated by sex for each one of the functional networks using healthy controls to create a baseline for the quality index and to exclude or keep the subjects on the basis of their motion. The data from healthy controls came from the Human Connectome Project[24] and Openneuro,[25] comprising 319 female subjects (mean age, 22.18 [SD, 25.19] years) and 482 male subjects (mean age, 25.05 [SD, 28.26] years). The number of found regions was defined as the regions with z values different from zero that survived the thresholding process. Missing regions were defined as the regions that have not been identified but do belong to the specific functional template mask. The number of extra regions was defined as regions that do not belong to the respective functional network template mask but were found.

$$\text{Regions (Belong Template Mask)} = \text{Regions (Found)} + \text{Regions (Missing)} - \text{Regions (Extra)}.$$

Statistical Analysis

Classification Analysis. The whole-brain connectivity parcellation comprises 832 ROIs. To avoid overfitting in the regression model, we selected 6 key networks for successful aging,[3-5] encompassing 397 distinct ROIs, with some ROIs overlapping the networks, including the DMN, SN, ECN-L, ECN-R, hippocampal, and language networks. Penalized regression analysis used these networks and within-network nodes to determine brain regions with statistical differences between superagers and cognitively average elderly controls.

Each of the ROIs, grouped within the specific 6 networks, was considered as a covariate in the penalized regression modeling in the following way: For a set of predictors $X = X_1, \ldots, X_N$ with p measurements taken on each, and the response variable y, regression allows estimation of the coefficients β_i in the following linear regression model:

$$y = x_1\beta_1 + \cdots x_N\beta_N = X\beta.$$

The ordinary least squares (OLS) regression finds a set of β_i that minimize the sum-squared approximation error $(y - x\beta)^2$. However, in general, OLS solutions are often unsatisfactory because there is not a unique solution when $p \gg n$, and it is difficult to pinpoint which predictors are most relevant to the response. Various regularization approaches have been proposed in order to handle "large- p, small-n" data sets and to avoid overfitting, such as LASSO (Least Absolute Shrinkage and Selection Operator) and ridge regression, or a combination of both. Elastic Net (EN) addresses these shortcomings since variable selection is embedded into their model-fitting process. These methods were previously applied to a similar problem, with results suggesting that the EN regression was a more robust approach to extreme correlations among the predictors.[26] Briefly, sparse regularization methods include the L1-norm regularization on the coefficients, which is known to produce sparse solutions, ie, solutions with many zeros, thus eliminating predictors that are not essential.

For the analysis here, we used the EN regression that finds an optimal solution to the OLS problem objective, augmented with additional regularization terms that include the sparsity-enforcing. Specifically, there are 2 types of regularizations that EN allows: L1-norm constraint on the regression coefficients that penalizes the absolute size and "shrinks" some coefficients to zero, and a "grouping" L2-norm constraint, which penalizes the squared size of the coefficients and enforces similar coefficients on predictors that are highly correlated with each other, which L1-constraint alone does not provide. Formally, EN regression optimizes the following function,

$$L(\lambda_1, \lambda_2; \beta) = (y - x\beta)^2 + \lambda_1\|\beta\|_1 + \lambda_2\|\beta\|_2,$$

where λ_1 is L1-penalty term and λ_2 is the quadratic penalty term.

In our case, for each of the networks, we let y be a binary outcome of either being a superager or an elderly control and X consisted of 397 covariate measurements representing the regions (nodes) across the 6 neural networks. We modeled the relationship as,

$$logit(p^i) = X^i\beta^i, \quad i = 1, 2, \ldots, n.$$

Model Prediction and Classification. Using these models, we calculated the expected probabilities of an individual being a superager predicted from the penalized regression model using the measurements of the network and plotted this as an outcome (on the y-axis) versus the binary observed values of the individual being either an elderly control or superager to evaluate the prediction performance of the model (Fig 2). The diagonal lines in Fig 2 represent the mean difference between predicted probabilities for superagers and elderly controls. The prediction model can be thought of as an OLS linear regression,

$$\underline{p}_{control} + (\underline{p}_{superager} - \underline{p}_{control})s,$$

where s is the observed data superager indicator variable, $\underline{p}_x$ is the mean predicted probability of being a superager for the observed group (either control or superager), and $\underline{p}_{superager} - \underline{p}_{control}$ is the slope of the line, which indicates the discriminatory ability of the model. Larger values demonstrate better performance (steeper lines), and zero corresponds to no predictive ability with a horizontal line for that network.

Quantification of Regression Analysis Results. We used the regression models in Equation $logit(p^i) = X^i\beta^i, \quad i = 1, 2, \ldots, n$ to infer the ORs describing the difference between the odds of exposure in each network and region (node) among superagers and elderly controls. In our study, they can be interpreted as a measure of the relative influence of a network and region within on the likelihood of being a superager. We obtained the ORs using the fitted models to give an average comparison between individuals with or without a unit increase in a particular region j; if p is the probability of being a superager then,

$$OR_j = \frac{p_j/(1-p_j)}{p/(1-p)} = exp(\beta_j).$$

We used the ORs to quantify the influence of each region within each of the 6 networks. We identified the regions with the

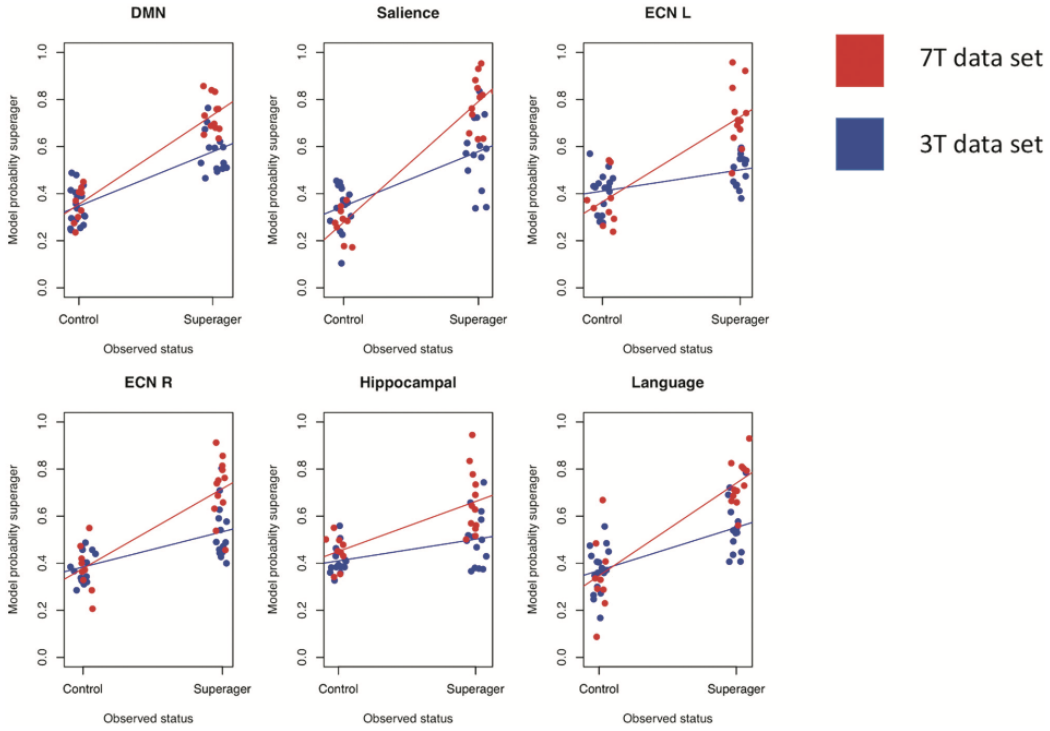

FIG 2. Plots showing the classification results for superagers across several networks examined on 3T and 7T fields. These plots show the observed superager status for each participant (*blue and red dots*) plotted against the probability of being a superager predicted from the fitted model. The *diagonal lines* represent the mean difference between predicted probabilities for superagers and elderly controls. The steeper the gradient of the lines, the higher the superagers' prediction.

ORs that are >1 to be the regions that are most differentiable/discriminative between superagers and elderly controls. If the OR values were equal to 1 (OR = 1), there was no discrimination in the examined regions between groups. Finally, if the OR values were <1, the regions negatively discriminated the examined region as characteristic for a superager. We noted that the *P* value was not generated from this analysis but the significance of the influence from a network/region could be inferred from the 95% CI for an OR.[27]

Because the number of variables in the model was very large, the maximum number of nonzero variables was limited to 10. For the analyses, we used the statistical programming language R (https://cran.r-project.org/web/packages/glmnet) and the package glmnet.[26]

RESULTS

Demographics and Neuropsychological Performance Scores

Superagers and elderly controls did not differ in terms of age (P = .304), education (P = .299), or sex distribution (P = .224). Superagers had statistically significantly better performance compared with elderly controls in the Montreal Cognitive Assessment (P = .003) and some episodic memory tests, including the Delayed-Recall Brief Cognitive Screening Battery (P = .036), Delayed-Recall Rey Auditory Verbal Learning Test (P < .001), and Logical Memory Delayed-Recall (P = .01) (Online Supplemental Data).

Discriminative Networks and Brain Nodes for Predicting Superagers

The lollipop plots (as an alternative to bar charts) in Fig 3 show the magnitude (dot) and the range (line) of the nodes within each network that are discriminative between superagers and elderly controls. Here ORs > 1 suggest nodes that are more likely to be different in superagers (ie, larger influence on the predicted probability of being a superager) and are illustrated by lollipops in green. Conversely, nodes with ORs < 1 are less likely to be different in superagers (ie, these regions are negatively discriminated as a characteristic of a superager) and are illustrated by lollipops in red.

When we used the 3T and 7T data sets, though all networks were overall distinct in superagers compared with elderly controls (Fig 2), some of them were more differentiable and predictive of superagers than others. For example, for the 3T data (Fig 3*A*), the ORs for the SN and language networks were >1 across some regions, with relatively good predictive performance (Fig 2), suggesting that these regions were discriminative in superagers. In contrast, the ECN-L presented only a few regions of ORs > 1 and others with ORs < 1, showing a poor predictive performance. For the 7T data analysis (Fig 3*B*), the lollipop plots in most

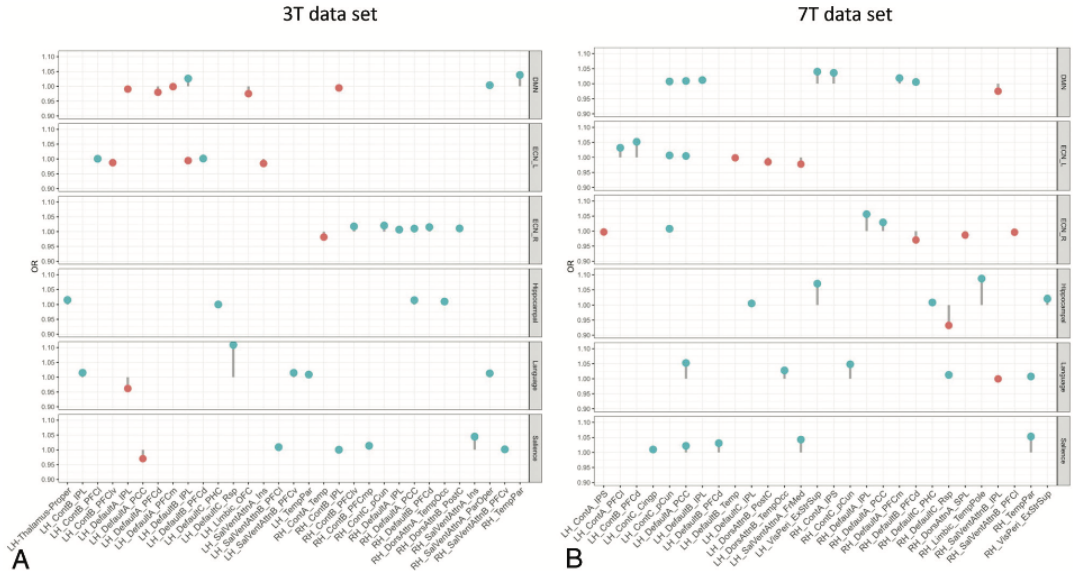

FIG 3. The *lollipop plots* in the 3T data set (*A*) and the 7T data set (*B*) indicate the nodes within networks that can differentiate superagers from elderly controls. Within the plots, we show the magnitude (*dot*) and the range (*line*) of the difference between superagers and elderly controls. ORs of >1 (OR > 1) suggest a larger influence on the predicted probability of being a superager (*lollipops in green*). ORs of < 1 indicate regions negatively discriminated as characteristic of a superager (*lollipops in red*). Cingp indicates posterior cingulate cortex; ContA, control A; ContB:, control B; ContC, control C; DorsAttnA, dorsal attention A; DorsAttnB, dorsal attention B; ExStrSup, extrastriate superior cortex; FrMed, frontal medial cortex; Ins, insula; IPL, inferior parietal lobule; IPS, intraparietal sulcus; LH, left hemisphere; OFC, orbital frontal cortex; ParOper, parietal operculum; PCC, precuneus posterior cingulate cortex; pCun, precuneus; PHC, parahippocampal cortex; PFCd, dorsal prefrontal cortex; PFCl, lateral prefrontal cortex; PFClv, lateral ventral prefrontal cortex; PFCm, medial prefrontal cortex; PFCmp, medial posterior prefrontal cortex; PFCv, ventral prefrontal cortex; PostC, postcentral cortex; RH, right hemisphere; Rsp, retrosplenial cortex; SalVentAttnA; salience/ventral attention A; SalVentAttnB, salience/ventral attention B; SPL, superior parietal lobule; Temp, temporal cortex; TempPar, temporoparietal junction; TempPole, medial temporal pole; TempOcc, temporo-occipital junction; VisPeri, peripheral visual.

networks had ORs > 1 across several nodes and great predictive performance, characterized by a steeper slope of the diagonal lines in Fig 2. The DMN, SN, hippocampal, and language networks were the most discriminative networks in our model prediction classifier for the 7T data set. In addition, for the 7T magnetic field, we had improved sensitivity in detecting a higher number of essential regions within each network. Therefore, on the basis of the classification algorithm, when differentiating superagers from elderly controls, we were more confident using the model fit from the 7T rather than the 3T scanner.

The Online Supplemental Data delineate the anatomic space of each network studied (networks masks). Figures 4, 5, and 6 illustrate the nodes within each network in brain maps, with OR values > 1, which predict superagers for the 3T and 7T data sets (Online Supplemental Data). We used Montreal Neurological Institute coordinates to plot the nodes and heatmaps, varying from dark blue to dark red (OR values furthest away from 1 have higher superager prediction), to demonstrate the discriminative power of each node. The Online Supplemental Data show the elastic model results for the 3T and 7T data sets for all ROIs included.

DISCUSSION

In this study, we identified functional networks showing that superagers exhibited distinct intrinsic connectivity compared with elderly controls in a range of brain networks and the core networks predicting a superager were the DMN, SN, and language. Areas in the precuneus posterior cingulate cortex, prefrontal cortex, temporoparietal junction, temporal pole, extrastriate superior cortex, and insula were the most discriminative nodes within these networks. By exploring the 7T and the 3T data sets separately, we could demonstrate higher prediction task confidence in rs-fMRI data sets acquired with the 7T rather than with the 3T scanner.

During the past years, clinical fMRI at 7T has gained traction[28] because it offers a beneficial increased SNR and BOLD contrast over conventional 1.5T and 3T MR imaging scanners,[29,30] translated into a greatly enhanced spatial resolution of functional activity, the main clinical advantage of 7T fMRI.[31,32] A prior study[33] demonstrated up to 300% improvement in the temporal SNR and resting-state functional connectivity coefficients provided by ultra-high-field 7T fMRI compared with 3T, indicating enhanced power for the detection of functional neural architecture. We have shown that the higher BOLD contrast-to-noise ratio available at 7T yielded improved sensitivity in detecting differences in the activity across all networks compared with the 3T field, reflected by a steeper gradient of the lines in the prediction classification algorithm. Moreover, higher ORs (OR > 1) were observed across several nodes for the 7T compared with the 3T data set. These differences imply that 7T scanners may facilitate

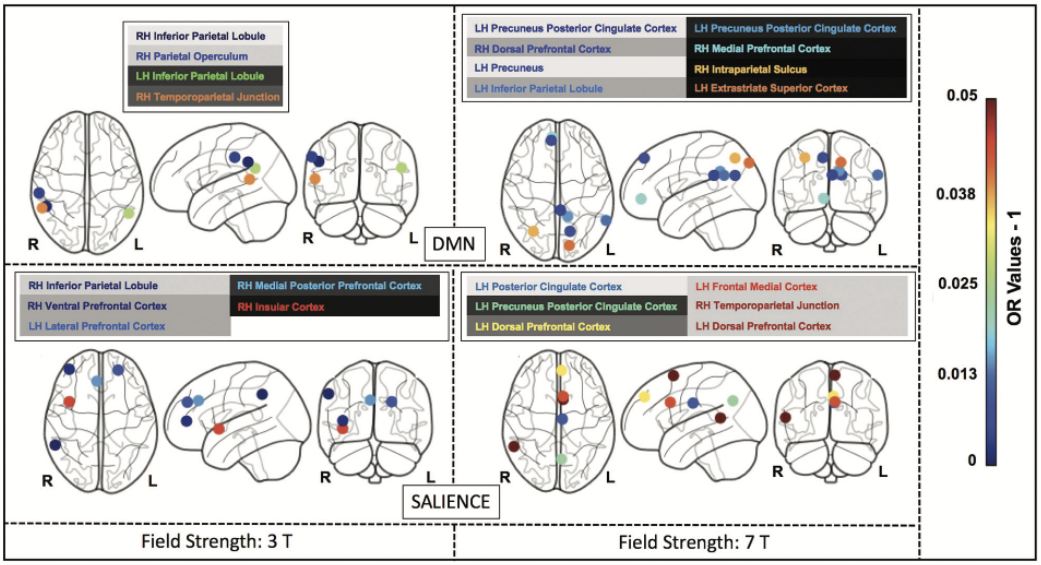

FIG 4. The most discriminative nodes among the DMN and SN in superagers compared with elderly controls. The heatmap varies from dark blue to dark red (denoting a higher prediction rate for classification as a superager using ORs). RH indicates right hemisphere; LH, left hemisphere; L, left; R, right.

high-quality connectivity measurements capturing stronger evoked rs-fMRI responses, hence offering potentially greater group-level power. This possibility raises our confidence for the results of the within-network nodes and overall model fit from the 7T scanner. Therefore, in the discussion below, the discriminatory nodes for identifying superagers at the 7T data set are emphasized more.

In line with previous studies including successful agers from 60 years of age,[4,34] we have found important features for predicting superagers in the DMN and SN. The DMN is implicated in memory encoding, storage, and retrieval, while the SN is believed to be associated with executive processes and detecting emotionally relevant stimuli, as well as alerting.[5] In parallel, normal aging is associated with decreased signal complexity within the DMN and SN nodes,[35] and there is a disrupted variability in these networks in mild cognitive impairment and Alzheimer disease.[36] It stands to reason that the DMN and SN hubs may potentially provide valid and reliable biomarkers for early age-related cognitive decline.

Beyond the classic hubs of the DMN and SN, we also found discriminative nodes within the ECN-L/R, language, and hippocampal networks for predicting a superager among elderly controls. The ECN is generally involved in tasks relying on executive functions, such as the control process and working memory.[37] The hippocampal network plays an important role in the consolidation of short-term memory and spatial memory.[38] The language network, a critical connectome in our model, encompasses regions of the Broca (inferior frontal) and Wernicke (superior temporal with extension into the inferior parietal cortex) areas[39] and has not been previously investigated in understanding the superior preservation of cognitive abilities. Although our groups did not show significant differences in verbal fluency tests, modifications in the language functional connectivity may anticipate changes in language performance in healthy older adults. Moreover, it is well-known that the language network can accurately discriminate patients with mild cognitive impairment from healthy controls[40] and is also known to demonstrate weaker functional connectivity in Alzheimer disease.[41]

The nodes with superior importance for predicting superagers encompassed areas in the extrastriate superior cortex, precuneus posterior cingulate cortex in both hemispheres; inferior parietal lobule, the temporoparietal junction, intraparietal sulcus, insula, and medial temporal pole in the right brain hemisphere; and the prefrontal/dorsal prefrontal cortex, temporo-occipital junction, and retrosplenial cortex in the left hemisphere. Most interesting, most of these cortical nodes presented with stronger intrinsic functional connectivity[4,34] and volumetric preservation,[5,42,43] akin to features of younger adults in previous studies.[3] These nodes also have been considered as key brain functional hubs for diverse cognitive functions and information integration among segregated functional networks.[44]

Our results indicate that the posterior cingulate cortex, a region mainly engaged in episodic memory,[45] plays a crucial role. Our previous study on superagers[10] showed a higher total NAA concentration in superagers than in elderly controls in the posterior cingulate cortex, reflecting a metabolically active brain region contributing to superior cognition in late life. Therefore, the functional and metabolic features of this structure observed in our cohort may underlie the superagers' significantly higher scores in the episodic memory tests. The prefrontal cortex, one of the most discriminative nodes in our cohort, is known to be associated with executive functions (planning, decision-making) and

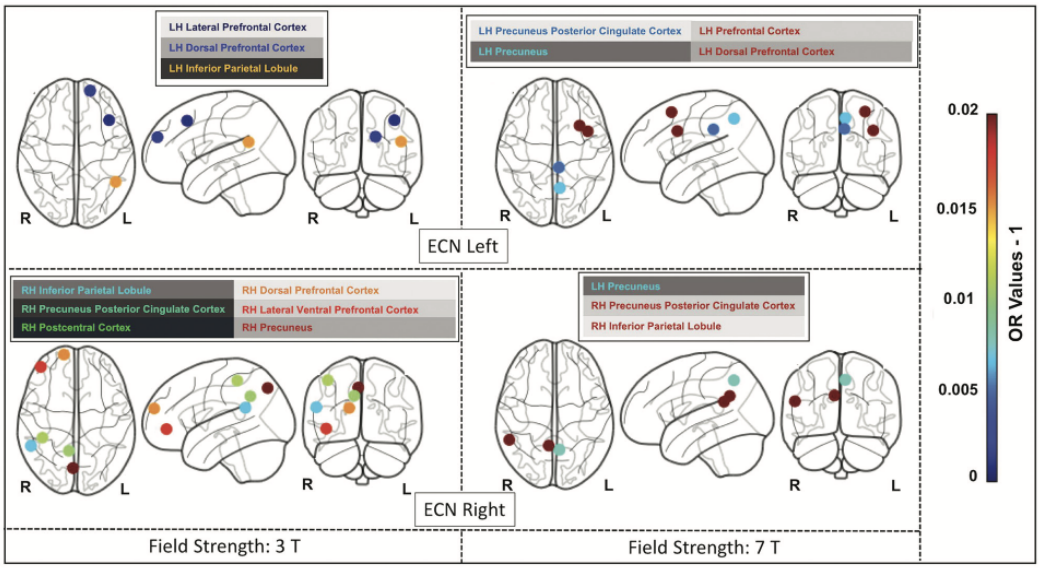

FIG 5. The most discriminative nodes among the ECN-L and ECN-R in superagers compared with elderly controls. The heatmap varies from dark blue to dark red (denoting a higher prediction rate for classification as a superager using ORs). RH indicates right hemisphere; LH, left hemisphere; L, left; R, right.

social-cognitive processes.[46] Another powerful discriminatory node, the right temporoparietal junction, is engaged in the social domain (empathy, sympathy) and self-evaluating behavior.[47] It was previously observed that superagers present with an increased level of positive relations with others, defined by truthfulness and satisfaction, and they manage stress better.[48]

Among the discriminative nodes from the classifier, the inferior parietal cortex is known to be involved in semantic processing and attention.[49] The insula contributes to various brain functions through the integration of sensory, emotional, and cognitive information.[50] Moreover, the extrastriate superior cortex, involved in visual-processing information, plays an important role in the DMN and hippocampal networks.[51] These nodes highlight how structures not directly involved with memory can contribute to superior memory performance.

Our study has a number of limitations. Our cohort was small due to the constraints in data collection and for prioritizing a rigorous selection protocol, preventing splitting the data set into training and validation samples. Also, the individuals scanned at 7T were a subset of those scanned at 3T due to patient contraindication heightened at 7T. Because for each individual, there were hundreds of measurements introducing a risk of overfitting, the penalized regression methodology was selected. The results should be seen as a contribution to the field and not definitive, because we aimed to investigate the signal that can be found in the data set in the presence of a low number of subjects and possible measurement error. The regression method used did not generate significant *P* values; however, even if we used standardized methodologies, these would have to be caveated. Moreover, we compared superagers with cognitively healthy older adults, reflecting early and subtle age-related cognitive functional changes; therefore, remarkable differences would not be expected.

The increased spatial resolution of BOLD on 7T and secondary higher detection of intrasubject variability can overestimate the intragroup differences in a small sample size.[52] There are also problems concerning B_0 and B_1 inhomogeneity created by higher field strengths, resulting in geometric distortion and drop-out, respectively, demanding advanced shimming and specialized pulse sequence designs.[53] The shorter TE (7T: 24 ms versus 3T: 30 ms), thinner slices (7T: 1.75 mm versus 3T: 3.6 mm), and parallel imaging can avoid some of these issues by reducing intravoxel inhomogeneity and through-plane dephasing.[53,54] The present study also had constraints regarding differences in acquisition protocols between the 3T and 7T scanners. First, the voxel size was different in 7T (isotropic voxel size = 1.75 mm^3) compared with 3T (voxel size = 3 × 3 × 3.6 mm). The precision of the whole-brain functional connectivity maps shown in this study may have been impacted by the smaller voxel size of the 7T protocol compared with 3T.[55] The TR was also longer at 3T (TR = 2000 ms) compared with 7T (TR = 1500 ms), indicating that the number of frames was higher for 7T for the same scan time. The higher number of frames is expected to improve the temporal resolution of the 7T scan compared with 3T. Ultimately, the acceleration factor was higher at 7T (multiband acceleration factor 3, IPAT 2) compared with 3T (ASSET factor 2.5), which can reduce signal distortion, signal drop-out, and partial volume effects but can also increase motion sensitivity and reduce the SNR.[29,56] Even though we highlight advancements in numerous metrics, including temporal SNR, sensitivity to detect connectivity measurements, and whole-brain connectivity maps for the data set at 7T compared with 3T, some results may be affected by differences in acquisition protocols and different scanners.

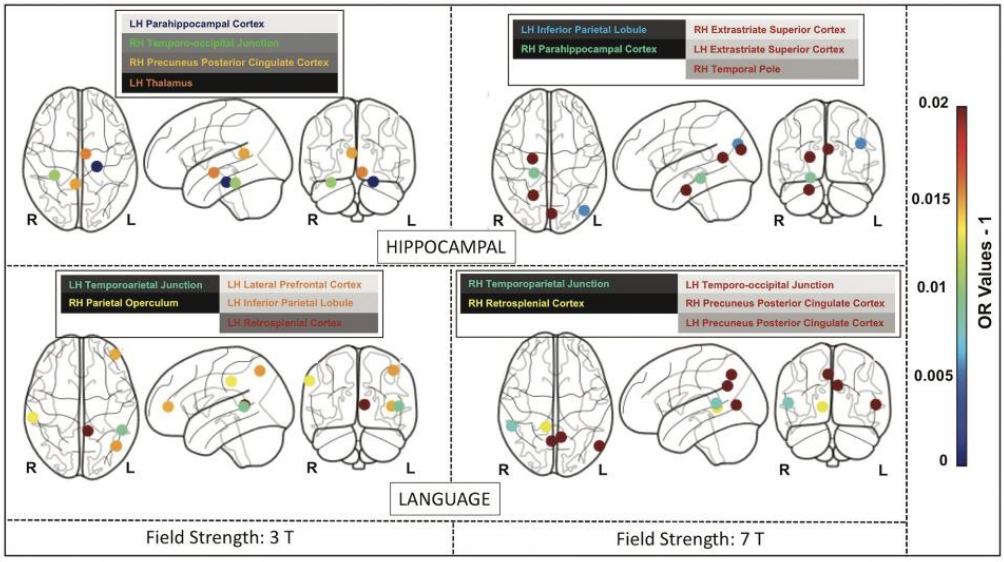

FIG 6. The most discriminative nodes among the hippocampal and language networks in superagers compared with elderly controls. The heat-map varies from dark blue to dark red (denoting a higher prediction rate for classification as a superager using ORs). RH indicates right hemisphere; LH, left hemisphere; L, left; R, right.

CONCLUSIONS

Our findings indicated that rs-fMRI may be a useful technique in assessing youthful memory performance in late life and identifying potential superagers, particularly in nodes among the DMN, SN, and language network. Our results highlight the benefit of 7T over the 3T magnetic field scanners for this diagnostic and classification task and warrant further validation in larger prospective studies.

ACKNOWLEDGMENTS

We thank Camila de Godoi Carneiro, MSc; Artur M. Coutinho, MD, PhD; and Carlos A. Buchpiguel, MD, PhD, for the collaboration in the development of this project.

Disclosure forms provided by the authors are available with the full text and PDF of this article at www.ajnr.org.

REFERENCES

1. Onoda K, Ishihara M, Yamaguchi S. **Decreased functional connectivity by aging is associated with cognitive decline.** *J Cogn Neurosci* 2012;24:2186–98 CrossRef Medline
2. Rogalski EJ, Gefen T, Shi J, et al. **Youthful memory capacity in old brains: anatomic and genetic clues from the Northwestern SuperAging Project.** *J Cogn Neurosci* 2013;25:29–36 CrossRef Medline
3. de Godoy LL, Alves CA, Saavedra JS, et al. **Understanding brain resilience in superagers: a systematic review.** *Neuroradiology* 2021;63:663–83 CrossRef Medline
4. Park CH, Kim BR, Park HK, et al. **Predicting superagers by machine learning classification based on the functional brain connectome using resting-state functional magnetic resonance imaging.** *Cereb Cortex* 2022;32:4183–90 CrossRef Medline
5. Sun FW, Stepanovic MR, Andreano J, et al. **Youthful brains in older adults: preserved neuroanatomy in the default mode and salience networks contributes to youthful memory in superaging.** *J Neurosci* 2016;36:9659–68 CrossRef Medline
6. Rogalski EJ. **Don't forget—age is a relevant variable in defining SuperAgers.** *Alzheimers Dement (Amst)* 2019;11:560–61 CrossRef Medline
7. Wang X, Ren P, Baran TM, et al; Alzheimer's Disease Neuroimaging Initiative. **Longitudinal functional brain mapping in supernormals.** *Cereb Cortex* 2019;29:242–52 CrossRef Medline
8. Mevel K, Chételat G, Eustache F, et al. **The default mode network in healthy aging and Alzheimer's disease.** *Int J Alzheimers Dis* 2011;2011:1–9 CrossRef Medline
9. Raimondo L, Oliveira ĹAF, Heij J, et al. **Advances in resting state fMRI acquisitions for functional connectomics.** *Neuroimage* 2021;243:118503 CrossRef Medline
10. de Godoy LL, Studart-Neto A, Wylezinska-Arridge M, et al. **The brain metabolic signature in superagers using in vivo ^{1}H-MRS: a pilot study.** *AJNR Am J Neuroradiol* 2021;42:1790–97 CrossRef Medline
11. Folstein MF, Folstein SE, McHugh PR. **Mini-Mental State: a practical guide for grading the mental state of patients for the clinician.** *J Psychiatr Res* 1975;12:189–98 CrossRef Medline
12. Brucki S, Nitrini R, Caramelli P, et al. **Suggestions for utilization of the Mini-Mental State Examination in Brazil** [in Portuguese]. *Arq Neuropsiquiatr* 2003;61:777–81 CrossRef Medline
13. Pfeffer RI, Kurosaki TT, Harrah CH Jr, et al. **Measurement of functional activities in older adults in the community.** *J Gerontol* 1982;37:323–29 CrossRef Medline
14. McKhann GM, Knopman DS, Chertkow H, et al. **The diagnosis of dementia due to Alzheimer's disease: recommendations from the National Institute on Aging-Alzheimer's Association workgroups on diagnostic guidelines for Alzheimer's disease.** *Alzheimers Dement* 2011;7:263–69 CrossRef Medline
15. Albert MS, DeKosky ST, Dickson D, et al. **The diagnosis of mild cognitive impairment due to Alzheimer's disease: recommendations from the National Institute on Aging-Alzheimer's Association workgroups on diagnostic guidelines for Alzheimer's disease.** *Alzheimers Dement* 2011;7:270–79 CrossRef Medline

16. Nitrini R, Caramelli P, Porto CS, et al. **Brief cognitive battery in the diagnosis of mild Alzheimer's disease in subjects with medium and high levels of education.** *Dement Neuropsychol* 2007;1:32–36 CrossRef Medline
17. Heaton RK, Miller SW, Taylor MJ, et al. **Revised comprehensive norms for an expanded Halstead-Reitan Battery: demographically adjusted neuropsychological norms for African American and Caucasian adults.** *PAR.* 2004. https://www.parinc.com/Products/Pkey/357. Accessed April 10, 2022
18. Shirk SD, Mitchell MB, Shaughnessy LW, et al. **A web-based normative calculator for the uniform data set (UDS) neuropsychological test battery.** *Alzheimers Res Ther* 2011;3:32 CrossRef Medline
19. Krafft O, Quick HH. **7T: Physics, safety, and potential clinical applications.** *J Magn Reson Imaging* 2017;46:1573–89 CrossRef Medline
20. Ribeiro de Paula D, Ziegler E, Abeyasinghe PM, et al. **A method for independent component graph analysis of resting-state fMRI.** *Brain Behav* 2017;7:e00626 CrossRef Medline
21. Nickerson LD, Smith SM, Öngür D, et al. **Using dual regression to investigate network shape and amplitude in functional connectivity analyses.** *Front Neurosci* 2017;11:115 CrossRef Medline
22. Schaefer A, Kong R, Gordon EM, et al. **Local-global parcellation of the human cerebral cortex from intrinsic functional connectivity MRI.** *Cereb Cortex* 2018;28:3095–114 CrossRef Medline
23. Bielczyk NZ, Llera A, Buitelaar JK, et al. **Increasing robustness of pairwise methods for effective connectivity in magnetic resonance imaging by using fractional moment series of BOLD signal distributions.** *Netw Neurosci* 2019;3:1009–37 CrossRef Medline
24. Van Essen DC, Smith SM, Barch DM, et al; WU-Minn HCP Consortium. **The WU-Minn Human Connectome Project: an overview.** *Neuroimage* 2013;80:62–79 CrossRef Medline
25. Snoek L, van der Miesen M, van der Leij A, et al. **AOMIC-PIOP1.** *Openneuro.* July 21, 2020. https://doi.org/10.18112/OPENNEURO.DS002785.V2.0.0. Accessed December 10, 2022
26. Friedman J, Hastie T, Tibshirani R. **Regularization paths for generalized linear models via coordinate descent.** *J Stat Softw* 2010;33:1–22 Medline
27. Bland JM, Altman DG. **Statistics notes: the odds ratio.** *BMJ* 2000;320:1468 CrossRef Medline
28. Isaacs BR, Mulder MJ, Groot JM, et al. **3 versus 7 Tesla magnetic resonance imaging for parcellations of subcortical brain structures in clinical settings.** *PLoS One* 2020;15:e0236208 CrossRef Medline
29. Beisteiner R, Robinson S, Wurnig M, et al. **Clinical fMRI: evidence for a 7T benefit over 3T.** *Neuroimage* 2011;57:1015–21 CrossRef Medline
30. van der Zwaag W, Francis S, Head K, et al. **fMRI at 1.5, 3 and 7 T: characterising BOLD signal changes.** *Neuroimage* 2009;47:1425–34 CrossRef Medline
31. Colizoli O, de Gee JW, van der Zwaag W, et al. **Comparing fMRI responses measured at 3 versus 7 Tesla across human cortex, striatum, and brainstem.** May 14, 2020. *bioRxiv*. https://doi.org/10.1101/2020.05.12.090175. Accessed April 15, 2022
32. Hale JR, Brookes MJ, Hall EL, et al. **Comparison of functional connectivity in default mode and sensorimotor networks at 3 and 7T.** *MAGMA* 2010;23:339–49 CrossRef Medline
33. Morris LS, Kundu P, Costi S, et al. **Ultra-high field MRI reveals mood-related circuit disturbances in depression: a comparison between 3-Tesla and 7-Tesla.** *Transl Psychiatry* 2019;9:94 CrossRef Medline
34. Zhang J, Andreano JM, Dickerson BC, et al. **Stronger functional connectivity in the default mode and salience networks is associated with youthful memory in superaging.** *Cereb Cortex* 2020;30:72–84 CrossRef Medline
35. Grady C, Sarraf S, Saverino C, et al. **Age differences in the functional interactions among the default, frontoparietal control, and dorsal attention networks.** *Neurobiol Aging* 2016;41:159–72 CrossRef Medline
36. Zhang L, Zuo XN, Ng KK, et al. **Distinct BOLD variability changes in the default mode and salience networks in Alzheimer's disease spectrum and associations with cognitive decline.** *Sci Rep* 2020;10:6457 CrossRef Medline
37. Wu L, Soder RB, Schoemaker D, et al. **Resting state executive control network adaptations in amnestic mild cognitive impairment.** *J Alzheimers Dis* 2014;40:993–1004 CrossRef Medline
38. Aertsen A. **Insights into hippocampal network function.** *Nat Comput Sci* 2021;1:782–83 CrossRef
39. Tomasi D, Volkow ND. **Resting functional connectivity of language networks: characterization and reproducibility.** *Mol Psychiatry* 2012;17:841–54 CrossRef Medline
40. Mueller KD, Koscik RL, Turkstra LS, et al. **Connected language in late middle-aged adults at risk for Alzheimer's disease.** *J Alzheimers Dis* 2016;54:1539–50 CrossRef Medline
41. Montembeault M, Chapleau M, Jarret J, et al. **Differential language network functional connectivity alterations in Alzheimer's disease and the semantic variant of primary progressive aphasia.** *Cortex* 2019;117:284–98 CrossRef Medline
42. Harrison TM, Maass A, Baker SL, et al. **Brain morphology, cognition, and β-amyloid in older adults with superior memory performance.** *Neurobiol Aging* 2018;67:162–70 CrossRef Medline
43. Gefen T, Peterson M, Papastefan ST, et al. **Morphometric and histologic substrates of cingulate integrity in elders with exceptional memory capacity.** *J Neurosci* 2015;35:1781–91 CrossRef Medline
44. van den Heuvel MP, Sporns O. **Network hubs in the human brain.** *Trends Cogn Sci* 2013;17:683–96 CrossRef Medline
45. Schneider F, Bermpohl F, Heinzel A, et al. **The resting brain and our self: self-relatedness modulates resting state neural activity in cortical midline structures.** *Neuroscience* 2008;157:120–31 CrossRef Medline
46. Amodio DM, Frith CD. **Meeting of minds: the medial frontal cortex and social cognition.** *Nat Rev Neurosci* 2006;7:268–77 CrossRef Medline
47. Krall SC, Rottschy C, Oberwelland E, et al. **The role of the right temporoparietal junction in attention and social interaction as revealed by ALE meta-analysis.** *Brain Struct Funct* 2015;220:587–604 CrossRef Medline
48. Cook Maher A, Kielb S, Loyer E, et al. **Psychological well-being in elderly adults with extraordinary episodic memory.** *PLoS One* 2017;12:e0186413 CrossRef Medline
49. Binder JR, Desai RH, Graves WW, et al. **Where is the semantic system? A critical review and meta-analysis of 120 functional neuroimaging studies.** *Cereb Cortex* 2009;19:2767–96 CrossRef Medline
50. La Corte V, Sperduti M, Malherbe C, et al. **Cognitive decline and reorganization of functional connectivity in healthy aging: the pivotal role of the salience network in the prediction of age and cognitive performances.** *Front Aging Neurosci* 2016;8:204 CrossRef Medline
51. Orban GA. **Higher order visual processing in macaque extrastriate cortex.** *Physiol Rev* 2008;88:59–89 CrossRef Medline
52. Jones SE, Lee J, Law M. **Neuroimaging at 3T vs 7T: is it really worth it?** *Magn Reson Imaging Clin N Am* 2021;29:1–12 CrossRef Medline
53. Balchandani P, Naidich TP. **Ultra-high-field MR neuroimaging.** *AJNR Am J Neuroradiol* 2015;36:1204–15 CrossRef Medline
54. Sladky R, Baldinger P, Kranz GS, et al. **High-resolution functional MRI of the human amygdala at 7 T.** *Eur J Radiol* 2013;82:728–33 CrossRef Medline
55. Newton AT, Rogers BP, Gore JC, et al. **Improving measurement of functional connectivity through decreasing partial volume effects at 7 T.** *Neuroimage* 2012;59:2511–17 CrossRef Medline
56. Vu AT, Jamison K, Glasser MF, et al. **Tradeoffs in pushing the spatial resolution of fMRI for the 7T Human Connectome Project.** *Neuroimage* 2017;154:23–32 CrossRef Medline

Supplementary Figure 1

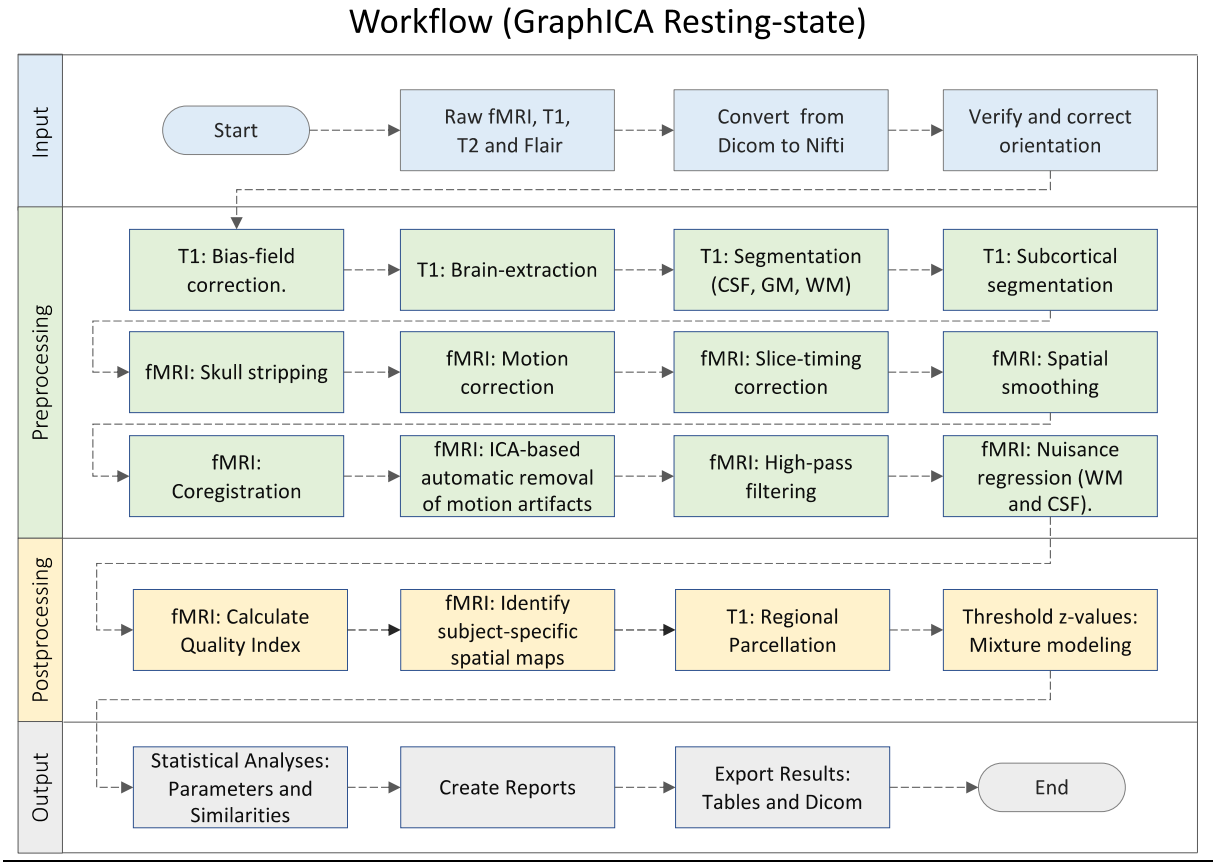

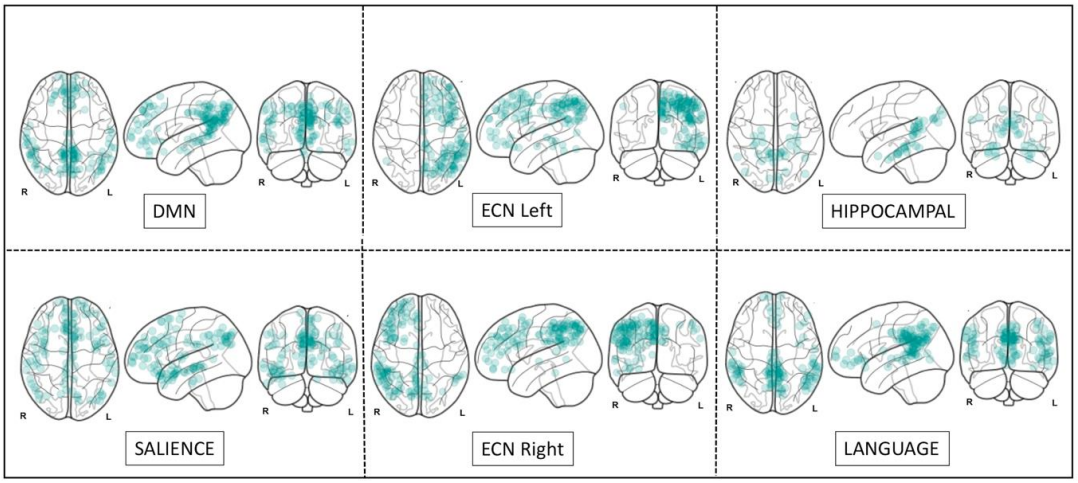

Supplementary Figure 2 – Networks Masks

Supplementary Table 1. Demographic information and neuropsychological test scores

	Elderly Controls (n = 17)		SuperAgers (n = 14)		p-value
	Mean (SD)	Median (IQR)	Mean (SD)	Median (IQR)	
Age (y)	84.47 (4.29)	84.00 (5.5)	82.93 (3.47)	81.50 (5.80)	0,304 [q]
Education (y)	14.88 (3.81)	16.00 (0.8)	15.93 (4.66)	16.00 (7.80)	0,299 [a]
Gender (%, male)	13 (76.50)		8 (57.10)		0,224 [b]
Psychiatric disorder (%)	1 (5.90)		1 (7.10)		0,708 [b]
Heart disease (%)	13 (25.50)		2 (14.30)		0,429 [b]
Hypothyroidism (%)	2 (11.80)		3 (25.00)		0,500 [b]
Dyslipidemia (%)	3 (25.00)		3 (21.40)		0,571 [b]
Diabetes mellitus (%)	3 (17.60)		3 (25.00)		0,500 [b]
Systemic arterial hypertension (%)	7 (41.30)		7 (50.00)		0,449 [b]
RAVLT Delayed-Recall [c]	6.00 (1.54)	6.00 (2.00)	10.93 (1.39)	11.50 (2.80)	**< 0,001 [a]**
MMSE [d]	28.58 (0.94)	29.00 (1.00)	29.00 (1.04)	29.00 (2.00)	0,260 [a]
MoCA [e]	24.06 (1.69)	24.00 (2.0)	26.50 (1.98)	27.00 (1.8)	0,003 [a]
BCSB Figure Memory Test Delayed Recall [f]	7.18 (1.77)	7.00 (3.80)	8.50 (1.16)	8.00 (2.00)	**0,036 [a]**
Clock Drawing Test	9.35 (0.86)	10.00 (1.80)	9.00 (2.08)	9.50 (1.00)	0,953 [a]
Verbal Fluency (animals)	17.17 (5.97)	16.00 (7.30)	19.79 (5.98)	18.00 (7.80)	0,128 [a]
Letter Verbal Fluency (FAS)	39.12 (13.04)	34.00 (18.30)	47.86 (13.94)	46.00 (19.80)	0,071 [a]
Logical Memory Delayed Recall	19.12 (7.47)	17.00 (11.00)	27.07 (6.94)	27.00 (5.80)	**0,01 [q]**
Rey Complex Figure (Copy)	33.32 (4.41)	34.00 (3.80)	35.64 (0.75)	36.00 (0.00)	**0,036 [a]**
Rey Complex Figure (Delayed-Recall)	11.97 (4.76)	11.00 (8.30)	15.14 (5.28)	16.00 (8.00)	0,084 [a]
Trail Making Test A	48.88 (12.77)	51.00 (16.30)	46.93 (13.55)	47.00 (22.50)	0,597 [a]
Trail Making Test B	119.53 (46.54)	113.00 (65.00)	108.29 (36.76)	107.00 (65.80)	0,544 [a]
Forward Digit Span	8.00 (2.37)	8.00 (3.00)	9.21 (2.26)	9.00 (2.80)	0,087 [a]
Backward Digit Span	5.29 (2.22)	5.00 (2.80)	6.07 (1.21)	6.00 (2.00)	0,161 [a]
BNT- 60 [g]	54.06 (5.15)	56.00 (8.00)	56.28 (3.65)	58.00 (6.50)	0,208 [a]

a. Mann-Whitney Test
b. Fisher's Exact Test
c. Rey Auditory Verbal Learning Test (RAVLT)
d. Mini Mental State Examination (MMSE)
e. Montreal Cognitive Assessment (MoCA)
f. Brief Cognitive Screening Battery (BCSB)
g. Boston Naming Test (BNT-60

Supplementary Table 2. Brain areas associated with the most discriminative nodes to predict superagers in a crescentic order.

Supplementary Table 2A

3 Tesla data set	
Target networks	**Brain areas**
DMN	R-inferior parietal lobule, R-parietal operculum, L-inferior parietal lobule, and R-**t**emporoparietal junction
SN	R-inferior parietal lobule, R-lateral ventral prefrontal cortex, L-lateral prefrontal cortex, R-medial posterior prefrontal cortex, and R-insula
ECN-L	L-lateral prefrontal cortex, L-dorsal prefrontal cortex, and L- inferior parietal lobule
ECN-R	**R**-inferior parietal lobule, R-precuneus posterior cingulate cortex, R-postcentral cortex, right dorsal prefrontal cortex, right lateral ventral prefrontal cortex, and right precuneus
Hippocampal network	L-parahippocampal cortex, R-temporo-occipital cortex, R-precuneus posterior cingulate cortex, and L-thalamus
Language network	L-temporoarietal junction, R-parietal operculum, L-lateral prefrontal cortex, L-inferior parietal lobule, and L-retrosplenial cortex

Supplementary Table 2B

7 Tesla data set	
Target networks	**Brain areas**
DMN	L-precuneus posterior cingulate cortex, R-dorsal prefrontal cortex, L-precuneus, L-inferior parietal lobule, L-precuneus posterior cingulate cortex, R-medial prefrontal cortex, R- intraparietal sulcus, and L-extra-striate superior cortex
SN	L- cingulate posterior cortex, L-precuneus posterior cingulate cortex, L-dorsal prefrontal cortex, L-frontal medial cortex, R-temporoparietal junction, and L-dorsal prefrontal cortex
ECN-L	L-precuneus posterior cingulate cortex, L-precuneus, L-prefrontal cortex, and L-dorsal prefrontal cortex
ECN-R	L-precuneus, R-precuneus posterior cingulate cortex, and R-inferior parietal lobule
Hippocampal network	L-inferior parietal lobule, R-parahippocampal cortex, R-extra-striate superior cortex, L-extra-striate superior cortex, and R-temporal pole
Language network	R-temporoparietal junction, R-retrosplenial cortex, L-temporo-occipital cortex, R-precuneus posterior cingulate cortex, and L-precuneus posterior cingulate cortex

Abbreviations: DMN = default mode network. ECN = executive control network. L = left. R = right. SN = salience network

Supplementary Table 3A: Elastic Net model results for 3T dataset

Network	Coefficient	Region	OR
DMN	-0.00940	LH_DefaultA_IPL_4	0.991
DMN	-0.02023	LH_DefaultA_PFCd_4	0.980
DMN	-0.00109	LH_DefaultA_PFCm_2	0.999
DMN	0.02590	LH_DefaultB_IPL_4	1.026
DMN	-0.02511	LH_Limbic_OFC_8	0.975
DMN	0.00072	RH_ContB_IPL_1	1.001
DMN	-0.01145	RH_ContB_IPL_3	0.989
DMN	0.00385	RH_SalVentAttnA_ParOper_9	1.004
DMN	0.03760	RH_TempPar_17	1.038
Salience	-0.01647	LH_DefaultA_PCC_15	0.984
Salience	-0.04445	LH_DefaultA_PCC_8	0.957
Salience	0.00900	LH_SalVentAttnB_PFCl_4	1.009
Salience	0.00031	RH_ContB_IPL_3	1.000
Salience	0.01378	RH_ContB_PFCmp_1	1.014
Salience	0.04346	RH_SalVentAttnA_Ins_4	1.044
Salience	0.00165	RH_SalVentAttnB_PFCv_2	1.002
ECN_L	0.00067	LH_ContB_PFCl_3	1.001
ECN_L	-0.01265	LH_ContB_PFClv_2	0.987
ECN_L	0.01485	LH_DefaultB_IPL_2	1.015
ECN_L	-0.02613	LH_DefaultB_IPL_4	0.974
ECN_L	0.00136	LH_DefaultB_PFCd_3	1.001
ECN_L	-0.01543	LH_SalVentAttnA_Ins_9	0.985
ECN_R	-0.01863	RH_ContA_Temp_3	0.982
ECN_R	0.01740	RH_ContB_PFClv_5	1.018
ECN_R	0.02024	RH_ContC_pCun_7	1.020
ECN_R	0.00671	RH_DefaultA_IPL_2	1.007
ECN_R	0.01021	RH_DefaultA_PCC_14	1.010
ECN_R	0.01509	RH_DefaultB_PFCd_1	1.015
ECN_R	0.01070	RH_DorsAttnB_PostC_8	1.011
Hippocampal	0.01530	LH-Thalamus-Proper	1.015
Hippocampal	0.00014	LH_DefaultC_PHC_3	1.000
Hippocampal	0.01462	RH_DefaultA_PCC_1	1.015
Hippocampal	0.01013	RH_DorsAttnA_TempOcc_2	1.010
Language	0.01476	LH_ContB_IPL_3	1.015
Language	-0.03900	LH_DefaultA_IPL_1	0.962
Language	0.10331	LH_DefaultC_Rsp_3	1.109
Language	0.01450	LH_SalVentAttnB_PFCv_5	1.015
Language	0.00882	LH_TempPar_9	1.009
Language	0.01280	RH_SalVentAttnA_ParOper_9	1.013

Supplementary Table 3B: Elastic Net model results for 7T dataset

Network	Coefficient	Region	OR
DMN	0.00748	LH_ContC_pCun_1	1.008
DMN	0.01390	LH_DefaultA_PCC_11	1.014
DMN	0.00457	LH_DefaultA_PCC_5	1.005
DMN	0.01215	LH_DefaultB_IPL_5	1.012
DMN	0.03941	LH_VisPeri_ExStrSup_22	1.040
DMN	0.03555	RH_ContA_IPS_6	1.036
DMN	0.01844	RH_DefaultA_PFCm_3	1.019
DMN	0.00573	RH_DefaultB_PFCd_5	1.006
DMN	-0.02510	RH_SalVentAttnB_IPL_1	0.975
Salience	0.00976	LH_ContC_Cingp_4	1.010
Salience	0.02176	LH_DefaultA_PCC_12	1.022
Salience	0.11712	LH_DefaultB_PFCd_11	1.124
Salience	-0.05892	LH_DefaultB_PFCd_2	0.943
Salience	0.03285	LH_DefaultB_PFCd_5	1.033
Salience	0.04197	LH_SalVentAttnA_FrMed_1	1.043
Salience	0.05142	RH_TempPar_1	1.053
ECN_L	0.03143	LH_ContA_PFCl_8	1.032
ECN_L	0.05059	LH_ContB_PFCd_1	1.052
ECN_L	0.00657	LH_ContC_pCun_10	1.007
ECN_L	0.00472	LH_DefaultA_PCC_13	1.005
ECN_L	-0.00140	LH_DefaultB_Temp_9	0.999
ECN_L	-0.01522	LH_DorsAttnB_PostC_3	0.985
ECN_L	-0.02242	LH_SalVentAttnA_FrMed_4	0.978
ECN_R	-0.00297	LH_ContA_IPS_4	0.997
ECN_R	0.00775	LH_ContC_pCun_10	1.008
ECN_R	0.05466	RH_DefaultA_IPL_2	1.056
ECN_R	0.02848	RH_DefaultA_PCC_6	1.029
ECN_R	-0.01389	RH_DefaultB_PFCd_3	0.986
ECN_R	-0.04601	RH_DefaultB_PFCd_6	0.955
ECN_R	-0.01337	RH_DorsAttnA_SPL_9	0.987
ECN_R	-0.00377	RH_SalVentAttnB_PFCl_2	0.996
Hippocampal	0.00542	LH_DefaultC_IPL_2	1.005
Hippocampal	0.06805	LH_VisPeri_ExStrSup_5	1.070
Hippocampal	0.00867	RH_DefaultC_PHC_4	1.009
Hippocampal	-0.07002	RH_DefaultC_Rsp_1	0.932
Hippocampal	0.08354	RH_Limbic_TempPole_12	1.087
Hippocampal	0.02057	RH_VisPeri_ExStrSup_2	1.021
Language	0.05127	LH_DefaultA_PCC_9	1.053
Language	0.02744	LH_DorsAttnB_TempOcc_1	1.028
Language	0.04698	RH_ContC_pCun_8	1.048
Language	0.01272	RH_DefaultC_Rsp_1	1.013
Language	-0.00037	RH_SalVentAttnB_IPL_1	1.000
Language	0.00751	RH_TempPar_15	1.008

Abbreviations:
Cingp: posterior cingulate cortex. **ContA:** control A. **ContB:** control B. **ContC:** control C. **DMN:** default mode network. **DorsAttnA:** dorsal attention A. **DorsAttnB:** dorsal attention B. **ExStrSup:** extra-striate superior cortex. **FrMed:** frontal medial cortex. **Ins:** Insula. **IPL:** inferior parietal lobule. **IPS:** intraparietal sulcus. **LH:** left hemisphere. **OFC:** orbital frontal cortex. **ParOper:** parietal operculum. **PCC:** Precuneus posterior cingulate cortex. **pCun**: precuneus. **PHC:** parahippocampal cortex. **PFCd:** dorsal prefrontal cortex. **PFCl:** lateral prefrontal cortex. **PFClv:** lateral ventral prefrontal cortex. **PFCm:** medial prefrontal cortex. **PFCmp:** medial posterior prefrontal cortex. **PFCv:** ventral prefrontal cortex. **PostC:** postcentral cortex**. RH:** right hemisphere. **Rsp:** retrosplenial cortex. **SalVentAttnA:** salience / ventral attention A. **SalVentAttnB:** salience / ventral attention B. **SPL:** superior parietal lobule. **Temp:** temporal cortex. **TempPar:** temporoparietal junction. **TempPole:** medial temporal pole. **TempOcc:** temporo-occipital junction. **VisPeri:** peripheral visual.

4 LIMITAÇÕES

4 LIMITAÇÕES

Nosso estudo tem uma série de limitações. Nossa coorte é pequena, devido às restrições no recrutamento de idosos acima de 80 anos cognitivamente preservados e por priorizar um protocolo de seleção rigoroso. Além disso, os dados publicados sobre a prevalência de superagers na população global ainda são insuficientes e não nos permitiram realizar uma análise de amostra antes da realização do estudo. A inclusão de grupos controle adicionais, como por exemplo adultos jovens e idosos com declínio cognitivo, poderiam ter ajudado a elucidar os achados metabólicas e funcionais nos superagers.

Em relação ao primeiro artigo publicado usando espectroscopia, as concentrações dos metabólitos examinados foram limitadas ao giro do cíngulo posterior; no entanto, as concentrações de metabólitos diferem entre regiões distintas do cérebro e entre a substância cinzenta e a branca, o que pode ter um impacto imprevisível no envelhecimento e nas assinaturas metabólicas dos superagers.

Referente ao segundo estudo em RM funcional, devido a coorte ser pequena não dividimos o conjunto de dados em amostras de treinamento e validação. Além disso, os indivíduos examinados na RM 7T foram um subconjunto daqueles examinados na RM 3T devido às contraindicações de medidas de segurança no campo magnético 7T. Como para cada indivíduo havia centenas de medidas que apresentavam risco de *"over-fitting"*, a metodologia de regressão penalizada foi selecionada. Os resultados devem ser vistos como uma contribuição para a área e não definitivos, pois pretendemos investigar o sinal que pode ser encontrado no conjunto de dados na presença de um baixo número de participantes e possível erro de medição. O método de regressão utilizado não gerou valores de p, porém, mesmo que utilizássemos metodologias padronizadas, ainda assim teríamos ressalvas.

5 CONCLUSÕES

5 CONCLUSÕES

1. Nossos estudos demonstraram com sucesso que técnicas multimodais avançadas de ressonância magnética do cérebro podem ajudar como biomarcadores adicionais não invasivos para diagnosticar o declínio cognitivo precoce e fornecer novos *insights* sobre os mecanismos biológicos envolvidos na resiliência cognitiva.
2. Demonstramos que a espectroscopia de prótons de voxel único por RM pode fornecer evidências *in vivo* de que o desempenho extraordinário da memória na senescência está positivamente associado ao NAA total no giro do cíngulo posterior. Esses achados apontam para a direção de que a concentração mais alta de NAA total (marcador de função neuronal e axonal) pode contribuir para o processo de resiliência das vias convencionais de envelhecimento presentes em superagers.
3. Nossos achados indicaram que a RM funcional de repouso pode ser uma técnica útil na avaliação do desempenho da memória excepcional em idosos e na identificação de potenciais superagers, particularmente nas respectivas redes funcionais, modo padrão, saliência e a rede de linguagem. Além disso, áreas no giro do cíngulo posterior, córtex pré-frontal, junção temporoparietal, pólo temporal, córtex extraestriado superior e ínsula foram as regiões mais discriminativas dentro das redes estudadas. Nossos resultados também destacaram potencial benefício da RM funcional no campo magnético 7T comparado ao aparelho de campo magnético 3T para a predição do perfil superager, principalmente devido a melhora substancial da relação sinal ruído, traduzida em uma resolução espacial aprimorada da atividade funcional.

6 ANEXOS

6 Anexo - PARECER CEP

USP - HOSPITAL DAS CLÍNICAS DA FACULDADE DE MEDICINA DA UNIVERSIDADE

PARECER CONSUBSTANCIADO DO CEP

DADOS DA EMENDA

Título da Pesquisa: ANÁLISE DE BIOMARCADORES DA DOENÇA DE ALZHEIMER EM UMA COORTE DE IDOSOS NORMAIS, COM DECLÍNIO COGNITIVO SUBJETIVO E COM DESEMPENHO EXCEPCIONAL DE MEMÓRIA.

Pesquisador: Ricardo Nitrini

Área Temática:

Versão: 3

CAAE: 62047616.0.0000.0068

Instituição Proponente: HOSPITAL DAS CLINICAS DA FACULDADE DE MEDICINA DA U S P

Patrocinador Principal: HOSPITAL DAS CLINICAS DA FACULDADE DE MEDICINA DA U S P
FUNDACAO DE AMPARO A PESQUISA DO ESTADO DE SAO PAULO

DADOS DO PARECER

Número do Parecer: 2.025.068

Apresentação do Projeto:

Trata-se de apresentação de emenda ao projeto original, datada de 02/04/2017, alterando apenas o que se refere ao tipo de equipamento de neuroimagem a ser utilizado (era Pet-CT e passa para Pet-RM). Estas informações foram atualizadas e constam da nova versão do TCLE.

Objetivo da Pesquisa:

Objetivo primário: Analisar e comparar a presença de biomarcadores da doença de Alzheimer (PET-CT com marcador amilóide, PET-CT com glicose marcada e ressonância magnética estrutural) em uma coorte de idosos normais, com declínio cognitivo subjetivo e com desempenho cognitivo excepcional ("SuperAgers" ou superidosos).Objetivos secundários:

Avaliar e comparar o desempenho longitudinal em testes neuropsicológicos, padronizados para idade e escolaridade, entre os três grupos citados em um seguimento anual por três anos.Correlacionar o desempenho longitudinal nas avaliações neuropsicológicas com a presença ou não de biomarcadores para doença de Alzheimer.•Analisar a sensibilidade da tarefa de memória integrativa (Short-Term Memory Binding - STMB) como marcador clínico de declínio cognitivo subjetivo e correlacioná-la com a presença de biomarcadores da doença de Alzheimer.•Classificar toda a amostra em quatro grupos conforme status de biomarcadores: negativo (A-/ND-),

Endereço: Rua Ovídio Pires de Campos, 225 5º andar
Bairro: Cerqueira Cesar **CEP:** 05.403-010
UF: SP **Município:** SAO PAULO
Telefone: (11)2661-7585 **Fax:** (11)2661-7585 **E-mail:** cappesq.adm@hc.fm.usp.br

amiloidose apenas (A+/ND-), amiloidose com neurodegeneração (A+/ND+) e suspeita de patologia não-Alzheimer (A-/ND+); e compará-los quanto ao declínio subjetivo e ao desempenho na avaliação neuropsicológica. •Analisar e comparar, entre os três grupos, as regiões anatômicas comumente com maior vulnerabilidade à patologia Alzheimer quanto à espessura cortical, metabolismo glicolítico e depósito de peptídeo amilóide. •Investigar se a presença do alelo 4 da APOE está relacionado com maior prevalência de declínio cognitivo subjetivo e com pior desempenho em testes neuropsicológicos.

Avaliação dos Riscos e Benefícios:

Trata-se de estudo de risco mínimo, associado à injeção do contraste para marcação de glicose e de beta amiloide e da própria realização da Ressonância magnética.

Benefícios: Diversos estudos vêm demonstrando que indivíduos com declínio cognitivo subjetivo experimentam maior risco de progressão para demência pela doença de Alzheimer. Adicionalmente, há evidências que esse grupo tem maior prevalência de biomarcadores positivos para amiloidose e neurodegeneração. Por consequência, esses achados fortalecem a idéia de que as queixas cognitivas subjetivas podem ser um marcador clínico precoce da patologia e corroboram com o melhor entendimento da história natural da doença de Alzheimer a partir de fases pré-demenciais. No entanto, ainda não há uma clareza quais as características do declínio cognitivo subjetivo que sugerem um estágio pré-clínico da doença de Alzheimer. E isso se deve em parte pela falta de um consenso sobre como avaliar o declínio cognitivo subjetivo. No outro lado do espectro da cognição em idosos, há aqueles cujo envelhecimento não é acompanhado por um declínio em suas habilidades cognitivas. Esse grupo, denominado como "superidosos" ou "SuperAgers", constituem-se de idosos octa e nonagenários cujo desempenho em testes de memória iguala-se a de
indivíduos 20 a 30 anos mais jovens. Embora haja poucos estudos, existem correlatos anatomopatológicos que possam estar associados a uma resiliência que esses idosos têm aos efeitos do envelhecimento normal. Portanto, este presente projeto propõe-se a colaborar com esse crescente conhecimento, fundamental para compreendermos os estágios iniciais da enfermidade e assim direcioná-los como alvos de futuras intervenções terapêuticas. Além disso, não há estudos publicados com a população brasileira com seguimento longitudinal de idosos saudáveis com declínio cognitivo subjetivo e que os correlacionasse com biomarcadores da doença de Alzheimer. Também faltam estudos comparando indivíduos com
declínio subjetivo com idosos com desempenho cognitivo excepcional. A amostra, embora constituída por idosos recrutados a partir de um ambulatório hospitalar, não será formada por

USP - HOSPITAL DAS CLÍNICAS DA FACULDADE DE MEDICINA DA UNIVERSIDADE

Continuação do Parecer: 2.025.068

sujeitos que procurarão serviço médico por queixa de memória e assim será possível a constituição de um grupo controle sem queixa e outro com declínio cognitivo e compará-los quanto ao desempenho em testes neuropsicológicos formais e quanto à positividade ou não dos biomarcadores para peptídeo amilóide e para injúria neuronal.

Comentários e Considerações sobre a Pesquisa:

A pesquisa é inovadora e interessante com Introdução e objetivos claros e metodologia adequada para o estudo.

Considerações sobre os Termos de apresentação obrigatória:

Adequados e de acordo com a emenda proposta.

Recomendações:

Não há.

Conclusões ou Pendências e Lista de Inadequações:

Sem pendências.

Considerações Finais a critério do CEP:

Este parecer foi elaborado baseado nos documentos abaixo relacionados:

Tipo Documento	Arquivo	Postagem	Autor	Situação
Informações Básicas do Projeto	PB_INFORMAÇÕES_BÁSICAS_881147_E2.pdf	11/04/2017 18:40:42		Aceito
Declaração de Pesquisadores	ricardoadalbertocartaadendo0001.pdf	09/04/2017 17:39:04	Ricardo Nitrini	Aceito
Declaração de Pesquisadores	ricardoadalbertoemendabiomarcadores0001.pdf	09/04/2017 17:38:48	Ricardo Nitrini	Aceito
Projeto Detalhado / Brochura Investigador	Projeto_Nitrini_Studart_Emenda02.docx	13/03/2017 18:07:09	Ricardo Nitrini	Aceito
TCLE / Termos de Assentimento / Justificativa de Ausência	TCLE_emenda02.docx	13/03/2017 18:06:50	Ricardo Nitrini	Aceito
Declaração de Pesquisadores	ricardoadalbertocartaadendo156770001.pdf	10/12/2016 18:18:03	Ricardo Nitrini	Aceito
Declaração de Pesquisadores	ricardoadalbertoemenda156770001.pdf	10/12/2016 18:17:47	Ricardo Nitrini	Aceito
TCLE / Termos de Assentimento / Justificativa de	TCLE_etapa_traducao_adaptacao.docx	10/12/2016 18:11:26	Ricardo Nitrini	Aceito

Endereço: Rua Ovídio Pires de Campos, 225 5º andar
Bairro: Cerqueira Cesar **CEP:** 05.403-010
UF: SP **Município:** SAO PAULO
Telefone: (11)2661-7585 **Fax:** (11)2661-7585 **E-mail:** cappesq.adm@hc.fm.usp.br

USP - HOSPITAL DAS CLÍNICAS DA FACULDADE DE MEDICINA DA UNIVERSIDADE

Continuação do Parecer: 2.025.068

Ausência	TCLE_etapa_traducao_adaptacao.docx	10/12/2016 18:11:26	Ricardo Nitrini	Aceito
Folha de Rosto	ricardoadalbertofr156770001.pdf	14/11/2016 17:00:56	Ricardo Nitrini	Aceito
Outros	ricardoadalbertocadastro156770001cappesq.pdf	14/11/2016 16:59:43	Ricardo Nitrini	Aceito
Declaração de Instituição e Infraestrutura	Modelo_Parque_de_Equipamentos.pdf	14/11/2016 16:58:42	Ricardo Nitrini	Aceito
Projeto Detalhado / Brochura Investigador	Projeto_Nitrini_Studart.docx	08/11/2016 00:20:30	Ricardo Nitrini	Aceito
TCLE / Termos de Assentimento / Justificativa de Ausência	TCLE_atualizado.docx	08/11/2016 00:20:11	Ricardo Nitrini	Aceito
Declaração de Instituição e Infraestrutura	APROVACAO_INRAD_045_2016_67.pdf	06/11/2016 22:48:13	Ricardo Nitrini	Aceito

Situação do Parecer:
Aprovado

Necessita Apreciação da CONEP:
Não

SAO PAULO, 20 de Abril de 2017

Assinado por:
ALFREDO JOSE MANSUR
(Coordenador)

Endereço: Rua Ovídio Pires de Campos, 225 5º andar
Bairro: Cerqueira Cesar **CEP:** 05.403-010
UF: SP **Município:** SAO PAULO
Telefone: (11)2661-7585 **Fax:** (11)2661-7585 **E-mail:** cappesq.adm@hc.fm.usp.br

7 REFERÊNCIAS

7 REFERÊNCIAS

1. Harrison TM, Weintraub S, Mesulam MM, Rogalski E. Superior memory and higher cortical volumes in unusually successful cognitive aging. J Int Neuropsychol Soc. 2012;18(6):1081-5.

2. Gefen T, Shaw E, Whitney K, Martersteck A, Stratton J, Rademaker A, Weintraub S, Mesulam MM, Rogalski E. Longitudinal neuropsychological performance of cognitive SuperAgers. J Am Geriatr Soc. 2014;62(8):1598-600.

3. Rogalski EJ, Gefen T, Shi J, Samimi M, Bigio E, Weintraub S, Geula C, Mesulam MM. Youthful memory capacity in old brains: anatomic and genetic clues from the Northwestern SuperAging Project. J Cogn Neurosci. 2013;25(1):29-36.

4. Gefen T, Peterson M, Papastefan ST, Martersteck A, Whitney K, Rademaker A, Bigio EH, Weintraub S, Rogalski E, Mesulam MM, Geula C. Morphometric and histologic substrates of cingulate integrity in elders with exceptional memory capacity. J Neurosci. 2015;35(4):1781-91.

5. de Godoy LL, Alves CAPF, Saavedra JSM, Studart-Neto A, Nitrini R, da Costa Leite C, Bisdas S. Understanding brain resilience in superagers: a systematic review. Neuroradiology. 2021;63(5):663-83.

6. Lin F, Ren P, Mapstone M, Meyers SP, Porsteinsson A, Baran TM; Alzheimer's Disease Neuroimaging Initiative. The cingulate cortex of older adults with excellent memory capacity. Cortex. 2017;86:83-92.

7. Baran TM, Lin FV; Alzheimer’s Disease Neuroimaging Initiative. Amyloid and FDG PET of successful cognitive aging: Global and cingulate-specific differences. J Alzheimers Dis. 2018;66(1):307-18.

8. Wang X, Ren P, Baran TM, Raizada RDS, Mapstone M, Lin F; Alzheimer's Disease Neuroimaging Initiative. Longitudinal functional brain mapping in supernormals. Cereb Cortex. 2019;29(1):242-52.

9. Dang C, Yassi N, Harrington KD, Xia Y, Lim YY, Ames D, Laws SM, Hickey M, Rainey-Smith S, Sohrabi HR, Doecke JD, Fripp J, Salvado O, Snyder PJ, Weinborn M, Villemagne VL, Rowe CC, Masters CL, Maruff P; AIBL Research Group. Rates of age- and amyloid β-associated cortical atrophy in older adults with superior memory performance. Alzheimers Dement (Amst). 2019;11:566-75.

10. Harrison TM, Maass A, Baker SL, Jagust WJ. Brain morphology, cognition, and β-amyloid in older adults with superior memory performance. Neurobiol Aging. 2018;67:162-70.

11. Yang Z, Wen W, Jiang J, Crawford JD, Reppermund S, Levitan C, Slavin MJ, Kochan NA, Richmond RL, Brodaty H, Trollor JN, Sachdev PS. Age-associated differences on structural brain MRI in nondemented individuals from 71 to 103 years. Neurobiol Aging. 2016;40:86-97.

12. Zhang J, Andreano JM, Dickerson BC, Touroutoglou A, Barrett LF. Stronger functional connectivity in the default mode and salience networks is associated with youthful memory in superaging. Cereb Cortex. 2020;30(1):72-84.

13. Park CH, Kim BR, Park HK, Lim SM, Kim E, Jeong JH, Kim GH. Predicting superagers by machine learning classification based on the functional brain connectome using resting-state functional magnetic resonance imaging. Cereb Cortex. 2022;32(19):4183-90.

14. Dekhtyar M, Papp KV, Buckley R, Jacobs HIL, Schultz AP, Johnson KA, Sperling RA, Rentz DM. Neuroimaging markers associated with maintenance of optimal memory performance in late-life. Neuropsychologia. 2017;100:164-70.

15. Gefen T, Papastefan ST, Rezvanian A, Bigio EH, Weintraub S, Rogalski E, Mesulam MM, Geula C. Von Economo neurons of the anterior cingulate across the lifespan and in Alzheimer's disease. Cortex. 2018;99:69-77.

16. Huentelman MJ, Piras IS, Siniard AL, De Both MD, Richholt RF, Balak CD, Jamshidi P, Bigio EH, Weintraub S, Loyer ET, Mesulam MM, Geula C, Rogalski EJ. Associations of *MAP2K3* gene variants with superior memory in superagers. Front Aging Neurosci. 2018;10:155.

17. Stern Y. Cognitive reserve. Neuropsychologia. 2009;47(10):2015-28.

18. Nyberg L, Lövdén M, Riklund K, Lindenberger U, Bäckman L. Memory aging and brain maintenance. Trends Cogn Sci. 2012;16(5):292-305.

19. Solé-Padullés C, Bartrés-Faz D, Junqué C, Vendrell P, Rami L, Clemente IC, Bosch B, Villar A, Bargalló N, Jurado MA, Barrios M, Molinuevo JL. Brain structure and function related to cognitive reserve variables in normal aging, mild cognitive impairment and Alzheimer's disease. Neurobiol Aging. 2009;30(7):1114-24.

20. Whalley LJ, Staff RT, Fox HC, Murray AD. Cerebral correlates of cognitive reserve. Psychiatry Res Neuroimaging. 2016;247:65-70.

21. Harrison SL, Sajjad A, Bramer WM, Ikram MA, Tiemeier H, Stephan BC. Exploring strategies to operationalize cognitive reserve: A systematic review of reviews. J Clin Exp Neuropsychol. 2015;37(3):253-64.

22. Steffener J, Stern Y. Exploring the neural basis of cognitive reserve in aging. Biochim Biophys Acta. 2012;1822(3):467-73.

23. Lee MR, Denic A, Hinton DJ, Mishra PK, Choi DS, Pirko I, Rodriguez M, Macura SI. Preclinical (1)H-MRS neurochemical profiling in neurological and psychiatric disorders. Bioanalysis. 2012;4(14):1787-804.

24. Jung RE, Gasparovic C, Chavez RS, Caprihan A, Barrow R, Yeo RA. Imaging intelligence with proton magnetic resonance spectroscopy. Intelligence. 2009;37(2):192-8.

25. Jung RE, Yeo RA, Chiulli SJ, Sibbitt WL Jr, Brooks WM. Myths of neuropsychology: intelligence, neurometabolism, and cognitive ability. Clin Neuropsychol. 2000;14(4):535-45.

26. Jung RE, Brooks WM, Yeo RA, Chiulli SJ, Weers DC, Sibbitt WL Jr. Biochemical markers of intelligence: a proton MR spectroscopy study of normal human brain. Proc Biol Sci. 1999;266(1426):1375-9.

27 Jung RE, Yeo RA, Love TM, Petropoulos H, Sibbitt WL Jr, Brooks WM. Biochemical markers of mood: a proton magnetic resonance spectroscopy study of normal human brain. Biol Psychiatry. 2002;51(3):224-9.

28. Jung RE, Gasparovic C, Chavez RS, Flores RA, Smith SM, Caprihan A, Yeo RA. Biochemical support for the "threshold" theory of creativity: a magnetic resonance spectroscopy study. J Neurosci. 2009;29(16):5319-25.

29. Ryman SG, Gasparovic C, Bedrick EJ, Flores RA, Marshall AN, Jung RE. Brain biochemistry and personality: a magnetic resonance spectroscopy study. PLoS One. 2011;6(11):e26758.

30. Harris JL, Yeh HW, Swerdlow RH, Choi IY, Lee P, Brooks WM. High-field proton magnetic resonance spectroscopy reveals metabolic effects of normal brain aging. Neurobiol Aging. 2014;35(7):1686-94.

31. Cleeland C, Pipingas A, Scholey A, White D. Neurochemical changes in the aging brain: A systematic review. Neurosci Biobehav Rev. 2019;98:306-19.

32. Raimondo L, Oliveira ĹAF, Heij J, Priovoulos N, Kundu P, Leoni RF, van der Zwaag W. Advances in resting state fMRI acquisitions for functional connectomics. Neuroimage. 2021;243:118503.

33. Isaacs BR, Mulder MJ, Groot JM, van Berendonk N, Lute N, Bazin PL, Forstmann BU, Alkemade A. 3 versus 7 Tesla magnetic resonance imaging for parcellations of subcortical brain structures in clinical settings. PLoS One. 2020;15(11):e0236208.

34. Beisteiner R, Robinson S, Wurnig M, Hilbert M, Merksa K, Rath J, Höllinger I, Klinger N, Marosi Ch, Trattnig S, Geissler A. Clinical fMRI: evidence for a 7T benefit over 3T. Neuroimage. 2011;57(3):1015-21.

35. van der Zwaag W, Francis S, Head K, Peters A, Gowland P, Morris P, Bowtell R. fMRI at 1.5, 3 and 7 T: characterizing BOLD signal changes. Neuroimage. 2009;47(4):1425-34.

36. Colizoli O, de Gee JW, van der Zwaag, Donner TH. Comparing fMRI responses measured at 3 versus 7 Tesla across human cortex, striatum, and brainstem. bioRxiv May 14, 2020. Preprint at: https://doi.org/10.1101/2020.05.12.090175.

37. Morris LS, Kundu P, Costi S, Collins A, Schneider M, Verma G, Balchandani P, Murrough JW. Ultra-high field MRI reveals mood-related circuit disturbances in depression: a comparison between 3-Tesla and 7-Tesla. Transl Psychiatry. 2019;9(1):94.